HIPK family kinases bind and regulate the function of the CCR4-NOT complex

Alfonso Rodriguez-Gil[1,2], Olesja Ritter[1,2], Juliane Hornung[1,2], Hilda Stekman[1], Marcus Krüger[3], Thomas Braun[3], Elisabeth Kremmer[4], Michael Kracht[5] and M. Lienhard SCHMITZ[1,6]

[1]Institute of Biochemistry, Medical Faculty, Friedrichstrasse 24, Justus-Liebig-University, D-35392 Giessen (Germany), Member of the German Center for Lung Research

[3]Max Planck Institute for Heart and Lung Research, Ludwigstrasse 43, D-61231 Bad Nauheim (Germany)

[4]Institute of Molecular Immunology, Helmholtz Center Munich, German Research Center for Environmental Health (GmbH), Marchioninistraße 25, D-81377 Munich (Germany)

[5]Rudolf-Buchheim-Institute of Pharmacology, Justus-Liebig-University Giessen, Schubertstrasse 81, D-35392 Giessen (Germany)

[6]corresponding author:
e-mail: lienhard.schmitz@biochemie.med.uni-giessen.de
phone +49-641-9947570
fax +49-641-9947589

[2]these authors contributed equally

Key Words: HIPK2, cell death, DNA single strand breaks, CCR4-NOT, chemotherapy

Running title: Control of HIPK2 levels by CCR4-NOT

Abstract

The serine/threonine kinase HIPK2 functions as a regulator of developmental processes and as a signal integrator of a wide variety of stress signals such as DNA damage, hypoxia and reactive oxygen intermediates. As the kinase is generated in a constitutively active form, its expression levels are restricted by a variety of different mechanisms. Here we identify the CCR4-NOT complex as a new regulator of HIPK2 abundance. Downregulation or knockout of the CCR4-NOT complex member CNOT2 leads to reduced HIPK2 protein levels without affecting the expression levels of HIPK1 or HIPK3. A fraction of all HIPK family members associates with the CCR4-NOT components CNOT2 and CNOT3. HIPKs also phosphorylate the CCR4-NOT complex, a feature that is shared with their yeast progenitor kinase YAK1. Functional assays reveal that HIPK2 and HIPK1 restrict CNOT2-dependent mRNA decay. HIPKs are well known regulators of transcription, but the mutual regulation between CCR4-NOT and HIPKs extends the regulatory potential of these kinases by enabling posttranscriptional gene regulation.

Abbreviations:

HIPKs, homeodomain-interacting protein kinases; PDCD4, Programmed cell death protein 4; C/EBP, CCAAT/enhancer-binding-protein; CBP, CREB-binding protein; SGs, stress granules; PBs, processing bodies; CCR4, Carbon catabolite repressor 4; NOT, negative on TATA; CRISPR, clustered regularly interspaced short palindromic repeats; CPT, camptothecin; DTBP, dimethyl dithiobispropionimidate; CDK11, cyclin dependent kinase 11; CBB, Coomassie brilliant blue; SUMO, small ubiquitin-related modifier; SENP1, sentrin-specific protease; ChIP-Seq, chromatin immunoprecipitation coupled to massively parallel sequencing; CtBP, C-terminal binding protein; MEFs, mouse embryonic fibroblasts; PI, propidium iodide; IP, immunoprecipitation.

Introduction

The evolutionary conserved family of homeodomain-interacting protein kinases (HIPKs) consists of four related kinases termed HIPK1 to HIPK4. HIPK1-3 share a similar basic architecture and contain an N-terminal kinase region followed by various other domains mediating binding to further proteins. HIPKs shape signaling pathways mediating the response to various stress signals including DNA damage, reactive oxygen species and hypoxia (Saul and Schmitz, 2013). The kinases typically mediate pro-apoptotic functions and contribute to cell killing after exposure of cells to endangering signals such as DNA damage (D'Orazi *et al.*, 2002; Hofmann *et al.*, 2002). Thus downregulation of HIPK2 and its absent pro-apoptotic function has been linked to chemotherapy resistance (Lin *et al.*, 2014). Biochemical experiments revealed the relevance of HIPK2 cis-autophosphorylation at Tyr354 and Ser357 in the activation loop for its kinase function (Saul *et al.*, 2013; Siepi *et al.*, 2013). This mechanism ensures that newly translated HIPK2 is already constitutively active even in the absence of triggering signals. The constitutive HIPK2 activity can be further augmented in response to external cues by kinases such as TGFβ-activated kinase 1 (TAK1) or c-Abl (Shang *et al.*, 2013; Reuven *et al.*, 2015). As HIPK2 is constitutively active after being synthesized at the ribosome, its protein amounts are strictly controlled by various mechanisms in order to prevent exaggerated expression that could be detrimental for the cell. This is achieved by several layers of regulation taking place at several levels including the control of HIPK2 translation and protein stability. The RNA-binding protein PDCD4 (programmed cell death protein 4) suppresses the translation of *Hipk2* mRNA and thus limits its *de novo* protein synthesis (Ohnheiser *et al.*, 2015). In addition, the protein levels of HIPK2 are tightly controlled by degradative ubiquitination employing at least four different ubiquitin E3 ligases and also caspase-mediated cleavage of the C-terminal autoinhibitory domain (Saul and Schmitz, 2013). The HIPKs are mainly found in nuclear bodies, but a fraction also occurs in cytosolic speckles (de la Vega *et al.*, 2011; van der Laden *et al.*, 2015). In the nucleus, HIPKs function as regulators of gene expression upon phosphorylation of transcription factors and transcription regulatory proteins (D'Orazi *et al.*, 2012; Schmitz *et al.*, 2014). Various HIPK family members show functional redundancy at the biochemical level, as seen by partially overlapping interaction partners (Kim *et al.*, 1998). The partial redundancy is also observed at the genetic level where the individual knockout of HIPK1 or HIPK2 results in viable mice, while the simultaneous knockout of both kinases leads to embryonic lethality (Isono *et al.*, 2006).

Synthesis and decay of mRNAs must be strictly controlled and coordinated to allow for mRNA and protein homeostasis. While various protein complexes mediate capping and polyadenylation of mRNAs, other protein complexes counteract these processes. Stress conditions such as virus infections lead to sequestering of mRNAs in ribonucleoprotein complexes known as stress granules (SGs) or processing bodies (PBs) to prevent translation (Aulas *et al.*, 2015). One important multi-protein complex affecting all major steps of mRNA metabolism is the CCR4 (carbon catabolite repressor 4)-NOT (Negative on TATA) complex.

This well conserved multi-subunit complex consists of scaffolding proteins and enzymatically active subunits. In the human CCR4-NOT complex, the proteins CNOT2, CNOT7, CNOT8 and CNOT9 interact with the scaffold protein CNOT1 (Lau *et al.*, 2009). The multi-protein assembly contains four deadenylases (CNOT6, CNOT6L, CNOT7 and CNOT8), but these are not bound simultaneously. CNOT7 and CNOT8 associate with the complex in a mutually exclusive fashion and either CNOT6 or CNOT6L associate only with complexes containing CNOT7 (Miller and Reese, 2012). The CNOT4 subunit has ubiquitin E3 ligase activity but associates only loosely with the entire CCR4-NOT complex (Lau *et al.*, 2009; Bartlam and Yamamoto, 2010). The catalytically inactive subunits are important for the integrity of the entire multi-protein complex (Russell *et al.*, 2002; Ito *et al.*, 2011). The CCR4-NOT complex is involved in virtually the entire spectrum of functions spanning the sequential process of gene expression from transcription to translation and even protein degradation. The CCR4-NOT complex regulates all steps of transcription ranging from transcription initiation to elongation and rescue of arrested RNA Polymerase II (Lemaire and Collart, 2000; Babbarwal *et al.*, 2014; Dutta *et al.*, 2015). Among the interactors of the CCR4-NOT complex are also several components of the inner nuclear basket of the nuclear pore complex, suggesting an interaction that takes place on the nuclear face of the nuclear pore complex where CCR4-NOT might escort mRNAs for nuclear export (Kerr *et al.*, 2011). The CCR4-NOT subunits with ribonuclease activities mediate deadenylation of mRNAs, which is the initial and often rate-limiting step in mRNA degradation, which then proceeds via de-capping and exonucleolytic degradation from the 5′ and 3′ ends (Tucker *et al.*, 2001; Maryati *et al.*, 2015). CNOT4 also plays a crucial role in co-translational quality control and is associated with polysomes. Gene deletion experiments showed the requirement of CNOT4 for global translational repression under conditions of nutritional limitations (Preissler *et al.*, 2015). The ribosome-associated NOT4 protein also participates in ubiquitination and degradation of aberrant peptides and contributes to the assembly of the 26S proteasome (Laribee *et al.*, 2007; Panasenko and Collart, 2011).

Here we identify CNOT2 and CNOT3 as new interaction partners for HIPKs to allow association of these kinases with the CCR4-NOT complex. Downregulation of CNOT2 by shRNAs or CRISPR (clustered regularly interspaced short palindromic repeats)-Cas9-mediated gene editing leads to reduced levels of the HIPK2 protein. Simultaneous downregulation of HIPK2 and the highly related kinase HIPK1 enhances CNOT2-dependent mRNA decay, allowing the coupling of HIPKs to posttranscriptional gene regulation.

Results

HIPKs directly bind to the CCR4-NOT complex

To identify new HIPK2 interaction partners, a yeast-two-hybrid screen was performed using a kinase inactive version of HIPK2 as a bait. Among the interactors we found several copies of CNOT2 (supplementary Fig. 1). To confirm this finding by an independent experimental approach, cells were transfected to express epitope-tagged versions of CNOT2 and HIPK2. Co-immunoprecipitations with specific antibodies allowed to detect CNOT2 in immunoprecipitates of HIPK2 (Fig. 1A), indicating an interaction between both proteins. To test whether this interaction also occurs in intact cells prior to their lysis, cells were treated with the membrane permeable cross-linking agent dimethyl dithiobispropionimidate (DTBP) which allows covalent cross-linking of interacting proteins located in very close proximity. Co-immunoprecipitation experiments detected a specific interaction between CNOT2 and HIPK2 (Fig. 1B), showing an association between the endogenous proteins. The intracellular localization of HIPK2 and CNOT2 was compared by immunofluorescence experiments. While CNOT2 localized to cytosolic speckles, the HIPK2 protein was mainly found in the nucleus and to a certain extent also in cytosolic structures (supplementary Fig. 2). This localization was not changed upon coexpression of both proteins together, but a minor

fraction of the kinase was found in cytoplasmic foci where it co-localized with CNOT2 (Fig. 1C). It was also tested whether the association between HIPK2 and CNOT2 might be changed upon stressors leading to the accumulation of untranslated mRNAs (Buchan and Parker, 2009; Houseley and Tollervey, 2009). HeLa cells expressing GFP-tagged HIPK2 and FLAG-tagged CNOT2 were treated with the oxidative stress inducer sodium arsenite or the translation inhibitors anisomycin and puromycin. Immunofluorescence analysis showed that all three agents did not change the degree of co-localization between both interactors. Puromycin and sodium arsenite caused a strong relocalisation of the interaction partners to cytosolic aggregates and to the perinuclear region, respectively (Fig. 1D). Since HIPK2 and CNOT2 co-localize in discrete cytoplasmic foci, it was interesting to test whether those dots match with known cytoplasmic structures such as SGs and PBs. Co-staining between HIPK2 and marker proteins for SGs (TIA1) and PBs (PAN3) showed no significant co-localization either under normal conditions (supplementary Fig. 3) or after treatment with anisomycin, puromycin or sodium arsenite (supplementary Fig. 4, 5). The CNOT2 protein showed no co-localization with TIA1 and only a partial colocalization with PAN3 (supplementary Fig. 6). Collectively these data show co-localization of HIPK2 with CNOT2-containing structures that do not overlap with SGs or PBs.

In order to determine the HIPK2 region mediating the interaction with CNOT2, deletion mutants of HIPK2 lacking either the N- or the C-terminus were examined for their ability to bind to CNOT2. Co-immunoprecipitation experiments showed that deletion of the C-terminal part still allowed for the protein/protein interaction (Fig. 2A), thus identifying the N-terminal part as the interacting region. As the binding region contains the evolutionary conserved kinase domain shared with the other HIPK family members, it was interesting to test whether also HIPK1 and HIPK3 have the ability to bind CNOT2. Co-immunoprecipitation experiments showed binding of the other HIPK family members to CNOT2 (Fig. 2B, C). Accordingly, also HIPK1 and HIPK3 co-localize with CNOT2 in cytoplasmic foci (Fig. 2D), thus defining CNOT2 as a shared substrate for the HIPKs.

Are the HIPKs associated only with the CNOT2 subunit or the complete CCR4-NOT complex? To address this question, binding of HIPK to other subunits of the CCR4-NOT complex was tested by co-immunoprecipitation experiments. As the deadenylases CNOT6 and CNOT6L are integral parts of the complex, they were expressed either alone or together with the three kinases in 293T cells. All immunoprecipitated HIPKs were found to interact with CNOT6 and CNOT6L (Fig. 2E), thus showing that the binding of HIPK family members occurs with the entire CCR4/NOT complex.

The evolutionary conserved C-terminal region of CNOT2 contains the SH3-like NOT-box, which was shown to be responsible for the direct association with other proteins such as the cyclin dependent kinase CDK11 (Shi and Nelson, 2005). To test a possible contribution of the NOT-box for the binding to HIPK2, a deletion mutant of CNOT2 (CNOT2 ΔNOT-box) was created and tested for interaction with HIPK2. Deletion of the NOT-box precluded interaction with HIPK2 (Fig. 3A) and also HIPK3 (Fig. 3B), indicating that this region is necessary for the efficient binding to HIPKs. Also the CNOT3 protein contains a NOT-box, therefore it was interesting to test its ability to bind to HIPK2. GST pulldown experiments showed that binding of HIPK2 to CNOT3 was even stronger than binding of the kinase to CNOT2 (Fig. 3C).

CNOT2 controls HIPK2 levels

In further experiments we noticed that shRNA-mediated depletion of CNOT2 resulted in markedly decreased HIPK2 protein levels (Fig. 4A). In contrast, the levels of HIPK1 and HIPK3 stayed unchanged, suggesting that CNOT2-mediated regulation occurs specifically for the HIPK2 protein. In order to confirm this finding by an independent experimental approach

we eliminated CNOT2 protein expression using the CRISPR-Cas9 system. Also these cells showed significantly reduced HIPK2 protein levels (Fig. 4A), thus corroborating the finding that impaired CNOT2 expression results in reduced HIPK2 protein levels. The analysis of relative mRNA levels by qPCR showed that CNOT2 downregulation caused only a slight reduction of HIPK2 mRNA levels (Fig. 4B). This reduction was only seen for some regions of the Hipk2 mRNA, suggesting that further mechanisms account for reduced HIPK2 protein levels. To test the effect of CNOT2 depletion on HIPK2 protein stability, protein synthesis was blocked with anisomycin in control cells or cells treated to downregulate CNOT2. The degradation rates of HIPK2 were comparable in control and CNOT2 knockdown cells (Fig. 4C), thus suggesting that reduced steady state HIPK2 protein levels are also due to impaired translation.

Camptothecin (CPT)-triggered cell death is regulated by HIPK2 and CNOT2

In a search for physiologically relevant modulators of CNOT2 expression we noticed in a database search that CPT, a topoisomerase I inhibitor that induces DNA damage, leads to impaired CNOT2 mRNA expression (GEO DataSet gds1453). To validate this finding, 293T cells were exposed to various concentrations of this chemotherapeutic agent and CNOT2 mRNA was quantified by qPCR. In agreement with the microarray data set the treatment of cells with CPT led to markedly reduced CNOT2 levels. Also the mRNA levels of HIPK2 decayed in the presence of CPT, while the transcript levels of HIPK1 and HIPK3 remained unaffected. (Fig. 5A). CPT also resulted in significantly reduced protein amounts of CNOT2 and of all three HIPK family members (Fig. 5B). As CNOT2 does not regulate HIPK1 and HIPK3 mRNA and protein levels, this CPT-mediated effect seems to be independent from CNOT2. It was then interesting to test the role of CNOT2 and HIPK2 in CPT-triggered cell death. Cells were transfected to express shRNAs specific for CNOT2 or HIPK2 or a scrambled control, followed by induction of cell death by CPT or the anticancer drug etoposide. HIPK2-depleted cells were protected from etoposide-induced death (Fig. 6A), as expected from published literature (Sakamoto *et al.*, 2010). In contrast, knockdown of HIPK2 sensitized cells to CPT-induced cell death, indicating an anti-apoptotic function of HIPK2 in response to this stimulus. Knockdown of CNOT2 increased CPT- and etoposide-triggered cell death (Fig. 6A), indicating an anti-apoptotic function of this protein. These pro- and anti-apoptotic functions of HIPK2 and CNOT2 were also reflected by an independent experimental approach at the level of caspase-activities (supplementary Fig. 7). To test whether the anti-apoptotic function of CNOT2 involves the depletion of HIPK2, CNOT2 knockdown cells were transfected to express GFP-tagged active and inactive versions of this kinase. CNOT2-dependent sensitization to CPT-induced cell death was not affected by HIPK2 (supplementary Fig. 8), indicating that CNOT2- and HIPK2-regulated pathways are not connected at the level of apoptosis induction. Similar results were obtained when HIPK2-deficient mouse embryonic fibroblasts (MEFs) and wildtype controls were compared for CPT- or H_2O_2-induced cell death (Fig. 6B,C), showing that the nature of the apoptotic stimulus dictates the functional role of HIPK2 in apoptosis.

HIPKs phosphorylate and regulate the CCR4-NOT complex

The co-expression of HIPKs together with CNOT2 frequently resulted in the occurrence of a slower migrating CNOT2 form (compare Fig. 2A), suggesting a possible posttranslational modification of CNOT2 by the kinases. To test whether HIPK2 can phosphorylate CNOT2, both proteins were co-expressed and cell lysates remained untreated or incubated with λ phosphatase. Analysis of the gel electrophoretic behavior of CNOT2 showed that the HIPK2-induced occurrence of a slower migrating CNOT2 form was not seen after phosphatase treatment (Fig. 7A), revealing a HIPK2-mediated phosphorylation event. We also observed that phosphorylation was strongly induced by HIPK3 and various deletion

mutants thereof in a kinase-dependent fashion (Fig. 7B). To identify HIPK-mediated CNOT2 phosphorylation by an unbiased approach, a mass spectrometric analysis was performed. 293T cells were transfected to express HA-CNOT2 alone or together with FLAG-HIPK3 or FLAG-HIPK2 ΔC which efficiently phosphorylates CNOT2, followed by purification of the CNOT2 protein by immunoprecipitation. After SDS-PAGE and Coomassie brilliant blue (CBB) staining of the precipitated protein (supplementary Fig. 9), the CNOT2 bands were excised, subjected to tryptic in-gel-digestion and high resolution mass spectrometric analysis. These experiments showed HIPK-mediated phosphorylation of 5 serines within the CNOT2 protein by both HIPK2 and HIPK3 (see supplementary Table 1 and the Andromeda score in supplementary Table 2). As schematically displayed in Fig. 7C, these sites cluster in the N-terminal portion of CNOT2. To test a possible function of these CNOT2 phosphorylations we performed tethering assays where CNOT2 was fused to the RNA-binding domain of the λN protein which allows binding to a luciferase-encoding mRNA containing several copies of λN-binding B boxes (Gehring *et al.*, 2008). Expression of λN-CNOT2 resulted in a dose-dependent reduction of luciferase activity, indicating mRNA decay (supplementary Fig. 10). This reduction was also mirrored at the level of mRNA, as revealed by qPCR (data not shown). To test a possible function of CNOT2 phosphorylation for this activity we generated phosphorylation-deficient (serine to alanine) or phosphorylation mimicking (serine to glutamic acid) CNOT2 mutants. Both mutants had largely unchanged activities in mRNA decay assays (supplementary Fig. 10), showing that at least CNOT2 activity is not affected by these phosphorylation events. As several HIPKs bind to the entire CCR4-NOT complex we wanted to test the impact of these kinases for mRNA decay in a more general approach. In order to circumvent the described functional redundancy between the kinases (Isono *et al.*, 2006) we created a cell line where HIPK2 was knocked out by CRISPR-Cas9 and HIPK1 was strongly downregulated by a doxycycline (dox)-inducible shRNA (Fig. 7D). Tethering assays showed that elimination of HIPK2 alone did not affect CNOT2-mediated mRNA degradation, while simultaneous interference with HIPK1 and HIPK2 expression resulted in an increased mRNA decay (Fig. 7E). These data suggest that HIPK1 and HIPK2 serve to restrict CCR4-NOT mRNA decay activity.

Discussion

Regulation of HIPK2 by the CCR4-NOT complex

This study shows a new mechanism allowing the regulation of HIPK2 amounts via the CCR4-NOT complex. It is not clear whether impaired HIPK2 expression can be really attributed to the CNOT2 subunit, as interference with CNOT2 expression also affected expression of CNOT1 (supplementary Fig. 11), CNOT3 (data not shown) and probably further subunits as well. Interference with CNOT2 expression affects HIPK2 mRNA levels only to a minor extent and leaves HIPK2 degradation unaffected. Thus the reduced HIPK2 protein amounts in the absence of CNOT2 are likely due to a mixture of impaired transcription and reduced *de novo* synthesis of HIPK2 at the ribosome. A further complication comes from the fact that the vast majority of HIPK2 mRNA is occurring in the recently discovered species of circular RNA (Jeck *et al.*, 2013), and it is unclear whether this circular RNA is translated into a protein. The molecular mechanism allowing decreased HIPK2 synthesis is not known and might involve further regulatory proteins such as PDCD4, which was recently identified as an antagonist of HIPK2 translation (Ohnheiser *et al.*, 2015). While previous data also showed a repressive function of the CCR4-NOT complex on the translation of several proteins (Cooke *et al.*, 2010; Zekri *et al.*, 2013), the data described here are compatible with a situation where HIPK2 protein translation is supported by a functional CCR4-NOT complex. Our immunofluorescence data suggest that only a minor fraction of HIPK proteins is found in association with the CCR4-NOT complex. HIPK2 is a mainly nuclear protein, but the fraction

of cytosolic HIPK2 proteins can be increased by removal of covalently bound SUMO (small ubiquitin-related modifier) or by acetylation of lysines contained in nuclear localization signal 1 (de la Vega *et al.*, 2011; de la Vega *et al.*, 2012). Similarly, also HIPK1 can be transported to the cytosol after removal of SUMO by the protease SENP1 (sentrin-specific protease) (Li *et al.*, 2008). HIPK2 and also the other family members HIPK1 and HIPK3 contact the CCR4-NOT complex by their highly homologous kinase domain. Direct binding was observed to the NOT-box containing proteins CNOT2 and CNOT3, which heterodimerize through their NOT-boxes to form an exposed surface that might provide a binding platform for interaction partners (Boland *et al.*, 2013), as schematically summarized in Fig. 8A.

An anti-apoptotic function of HIPK2: implications for tumor therapy

A large set of studies described a pro-apoptotic function of HIPK2 in response to many different agents such as UV radiation, doxorubicin and etoposide (D'Orazi *et al.*, 2012; Hofmann *et al.*, 2013; Schmitz *et al.*, 2014). The ability of HIPK2 to induce cell death relies on p53-dependent and -independent pathways. HIPK2-mediated p53-dependent apoptosis critically involves p53 Ser46 phosphorylation, which in turn allows recruitment of the acetylase CBP to acetylate p53 at Lys382 (D'Orazi *et al.*, 2002; Hofmann *et al.*, 2002). The p53 Ser46 phosphorylation affects cell cycle modulatory genes only to a minor extent, while it preferentially activates pro-apoptotic p53 target genes, as revealed by gene array and ChIP-Seq (chromatin immunoprecipitation (ChIP) coupled to massively parallel sequencing) experiments (Smeenk *et al.*, 2011). But HIPK2 can also trigger cell death via p53-independent cell death pathways. These processes involve for example HIPK2-mediated phosphorylation of the anti-apoptotic transcriptional corepressor CtBP (C-terminal binding protein) (Zhang *et al.*, 2005) or phosphorylation of ΔNp63α, a dominant negative isoform of the p53 family member p63 (Lazzari *et al.*, 2011).

Here we reveal for the first time an anti-apoptotic function of HIPK2, implying that HIPK2 plays a dual role in the regulation of cell death, as shown schematically in Fig. 8B. Also other apoptosis regulators can have such a dual role, as seen in the case of p53 which is typically pro-apoptotic, but in some cases functions to prevent cell death (Lassus *et al.*, 1996; Vousden, 2006). Another example is provided by the largely anti-apoptotic transcription factor NF-κB that can also promote apoptosis dependent on the cell type and apoptotic stimulus (Dumont *et al.*, 1999; Radhakrishnan and Kamalakaran, 2006). CPT is a quinoline alkaloid which binds to DNA and the water soluble CPT derivatives Topotecan and Irinotecan are clinically used for the treatment of cancer (Houghton *et al.*, 1995). It will thus be very relevant to investigate in future studies whether also the efficacy of these drugs or further clinically used topoisomerase I inhibitors are limited by the anti-apoptotic function of HIPK2. In such a case the reduced HIPK2 amounts would still be sufficient to protect from the early steps of CPT-induced cell death and kinase inhibitors would be beneficial to increase the efficacy of chemotherapeutic treatment.

Regulation of CCR4-NOT by HIPKs?

As the CCR4-NOT complex has been identified as a central integration point coordinating virtually all different aspects of gene expression, it is important to control its functions and activities (Miller and Reese, 2012). Thus the composition of the CCR4-NOT complex is dynamic and individual subunits might function both within and outside of the complex in different cellular compartments (Collart and Panasenko, 2012). In addition, the relative expression levels of subunits can change, as exemplified by the downregulation of yeast CNOT1 in the absence of glucose (Norbeck, 2008) and the reduced expression of CNOT2 in the presence of CPT (this study). The complex is also regulated by different posttranslational modifications such as phosphorylation (Lau *et al.*, 2010). Here we identify 5 HIPK-mediated phosphorylation sites in CNOT2, but it is highly probable that these kinases also modify other

subunits of the complex. It remains to be seen whether the restriction of CNOT2 activity by HIPK1/2 is due to kinase-independent events or to regulatory phosphorylations. Interestingly, also the YAK1 kinase from yeast, a phylogenetic ancestor of the HIPK family, was shown to phosphorylate POP2/CAF1, a homologue of the human CNOT7 protein upon glucose limitation (Moriya *et al.*, 2001). YAK1 also associates with other components of this complex such as cell division cycle (CDC)39/NOT1 (http://www.yeastgenome.org/). It will thus be very interesting to study the functional consequences of CCR4-NOT phosphorylations in the future after comprehensively mapping basal and stimulus-regulated HIPK-dependent phosphorylation sites in this complex.

Materials & Methods

Antibodies, plasmids and reagents

All the information is given in the supplementary Table 3.

Cell culture and transfections

Human embryonic kidney HEK293T cells, HeLa, *HIPK2*$^{-/-}$ and control MEFs were grown in DMEM containing 10% FCS and 1% (w/v) penicillin/streptomycin at 37^{o}C and 5% CO_2. Cells were seeded in dishes and transfected using the transfection reagents Rotifect (Roth) or linear polyethylenimine. After pipetting up and down several times, complex formation occurred in serum- and antibiotic-free DMEM during 20 min at room temperature. After adding the transfection mixture to antibiotic-free DMEM containing FCS, the cells were incubated 3-5 h before the medium was changed and the cells were further grown. Stable cell clones containing the pINDUCER plasmids were produced by selection for 10 days in puromycin, followed by single clone picking and analysis of doxycycline-dependent protein and mRNA expression.

Cell lysis

To prepare cell extracts under native conditions, the cells were washed once with 1x PBS, harvested by scraping and collected by centrifugation for 4 min at 350 x g. The pellet was resuspended in an appropriate amount of NP-40 buffer (20 mM Tris/HCl pH 7.5, 150 mM NaCl, 1 mM phenylmethylsulfonylfluoride, 10 mM NaF, 0.5 mM sodium orthovanadate, leupeptine (10 µg/ml), aprotinin (10 µg/ml), 1% NP-40 and 10% glycerol) and incubated on ice for 20 min. The lysate was cleared by centrifugation for 10 min at 16000 x g. The supernatant was then used for immunoprecipitation experiments or mixed with 5x SDS sample buffer, boiled at 95°C for 5 min and analyzed by Western blotting. Alternatively cells were directly lysed in 1x SDS sample buffer, sonified to shear the genomic DNA and used for Western blotting.

Immunoprecipitation and Western blotting

Co-immunoprecipitation was either done after crosslinking of proteins with the membrane permeable crosslinker DTBP as described (Renner *et al.*, 2011) or after lysis of cells under native conditions using NP-40 buffer. The lysate was cleared by centrifugation at 12000 x g for 10 min. The supernatant was transferred to a fresh tube, 10% of the volume was removed as input sample, mixed with 5x SDS sample buffer and heated at 95°C for 5 min. The remaining lysate was pre-cleared by the addition of 20 µl of A/G-agarose bead slurry and incubation for 1 h at 4°C. Following centrifugation the pre-cleared lysate was transferred to a new tube and 1 µg of the precipitating antibody or control IgG was added. After incubation at 4°C for at least two h, 30 µl of A/G-agarose bead slurry was added and the lysates were incubated for another h at 4°C. In order to remove all proteins that were not precipitated, the beads were washed five times for 10 min with NP-40 buffer. After elution in 1,5x SDS sample buffer the samples were analyzed by Western blotting. This was done by separation of

proteins via SDS-PAGE, followed by semidry blotting to a polyvinylidene difluoride membrane (Millipore) as previously described (Milanovic *et al.*, 2014).

Immunofluorescence

Cells were grown in 12-well plates on cover slips, washed once with cold 1x PBS and fixed for one minute with an ice-cold methanol:acetone (1:1) solution. The fixing solution was aspirated off, the cells were rehydrated with 1x PBS for 10 min and then blocked for 60 min with 1x PBS containing 10% (v/v) goat serum. Afterwards the cells were incubated with the primary antibody diluted in 1x PBS containing 1% (v/v) goat serum either overnight at 4°C or for 2 h at room temperature. The cells were then washed three times for 5 min with 1x PBS and incubated with the appropriate secondary dye-coupled antibody diluted in 1x PBS containing 1% (v/v) goat serum for 2 h in the dark. The incubation was followed by three washing steps for 5 min with 1x PBS. Nuclear DNA was stained by incubating the cells with Hoechst 33324 for 5 min. Cells were again washed three times for 5 min and then mounted on microscope slides with Kaiser's glycerol gelatine. The stained proteins were analyzed using an inverted Nikon Eclipse 2000E microscope.

Tethering assays

A Renilla luciferase reporter construct harboring 5 B-box elements in its 3´ UTR was coexpressed with the B-box RNA-binding bacteriophage λN protein to tether the CNOT2 protein to the reporter mRNA. The reporter gene was coexpressed together with the λN fusion protein and the Firefly luciferase lacking B-box motifs as an internal control for normalisation. Transfections were done in 6-well plates and 24 h later cell lysates were prepared. The emitted bioluminescence was detected with a Berthold DuoLumat LB 9501 luminometer. The relative activities were calculated after the normalization of the Renilla luciferase activities to the activities of the Firefly luciferase.

GST-pull down experiments

GST fusion proteins were produced and purified from *E. coli.* The GSH sepharose beads containing the attached GST fusion proteins were washed with PBS and then incubated with 100 µl of NP-40 extracts containing the GFP-HIPK2 protein. Another 500 µl of NP-40 buffer was added and incubated on a rotating device for at least 4 h at 4°C. The beads were washed five times in NP-40 lysis buffer. Bound proteins were eluted by the addition of 40 µl 1,5x SDS sample buffer and subsequent boiling for 5 min. Proteins associated with GST fusion proteins were analyzed by Western blotting, while the recombinant GST proteins were controlled by SDS-PAGE and CBB staining.

Identification of CNOT2 phosphorylation sites by mass spectrometry

293T cells were transfected to express HA-CNOT2 alone or together with FLAG-HIPK2 ΔC or FLAG-HIPK3 and the CNOT2 protein was purified by immunoprecipitation using anti-HA antibodies. The CNOT2 bands were excised from the Coomassie-stained gel and subjected to tryptic in-gel-digestion. Extracted peptides were desalted using C18-based Stop and Go Extraction Tips and mass spectrometric measurements were performed with a nano liquid chromatography (LC) system, which was coupled to a LTQ-Orbitrap Velos mass spectrometer (Thermo Fisher Scientific) via a nanoelectrospray source (Proxeon) as described in (Hölper *et al.*, 2015). For mass spectrometric measurements, full MS scan spectra (m/z = 300–1650) were acquired in the Orbitrap with a resolution of R = 60,000 after accumulation of 1,000,000 ions. The 15 most intense peaks from full MS scan were isolated and fragmented in the linear ion trap after accumulation of 5,000 ions. Fragmentation of precursor ions was performed using CID (35% normalized collision energy) prior to acquisition of MS/MS scan spectra. The raw data were processed and analysed using the MaxQuant (Cox and Mann,

2008) software (version 1.2.2.9) and peptides were searched against a human FASTA database (version 3.68). Enzyme specificity was set to Trypsin with an additional allowance of cleavage N-terminal to proline. A maximum of 2 missed cleavages were allowed. Cysteine carbamidomethylation was set as fixed modification; and oxidation of methionine, acetylation of protein N-terminus and phosphorylation of STY (Serine, Threonine, and Tyrosine) were set as variable modifications. The initial precursor ion mass deviation was set to 7 ppm and the maximum allowed mass deviation was set to 20 ppm. MS/MS tolerance was set to 0.5 Da. A false discovery rate of 0.01 and minimum peptide length of 7 amino acids were used for peptide identifications.

CRISPR-Cas9-mediated gene targeting

Oligos targeting the first exon of the *CNOT2* or *Hipk2* genes were cloned into pX459 (Addgene) to obtain the pX459-CNOT2 and pX459-HIPK2 plasmids. 293T cells were transfected either with pX459 targeting the luciferase gene or pX459-CNOT2 and HeLa cells were transfected with the plasmid pX459-HIPK2. The next day puromycin (1 μg/ml) was added for 3 days to kill the untransfected cells. Single cell clones were isolated and tested for expression of the CNOT2 or HIPK2 proteins and Cas9 by Western blotting. Cells neither expressing CNOT2 or HIPK2 and also lacking Cas9 expression were used for the subsequent experiments. The Indel mutations in the knockout clones were characterized by sequencing of the genonic DNA.

Quantitative real-time PCR

The RNeasy mini kit (Qiagen) was used to extract total RNA from cells and RNA quality was tested on ethidium bromide-stained agarose gels. cDNA was synthesized using Oligo (dT) 20 primers and the Superscript II first strand synthesis system (Invitrogen). Real-time PCR was performed using Absolute SYBR Green ROX Mix (Thermo Scientific) with specific primers (supplementary table 3). Gene expression was determined using an Applied Biosystems 7300 real time PCR system, all experiments were performed in triplicates and quantification was done using the comparative $\Delta\Delta C_T$-method. For that, data were normalized to the housekeeping gene β-actin and the resulting ΔC_T values were compared to a sample that was chosen as a calibrator. The relative expression level was then calculated according to the following formula: $R = 2^{-\Delta\Delta CT}$.

Measurement of apoptosis

Apoptosis was measured by double staining with FITC-Annexin V and propidium iodide (PI) to allow distinguishing between cells in early apoptosis (FITC-Annexin V positive/PI negative) or late apoptotic stages (FITC-Annexin V positive/PI positive). The staining was performed using the Annexin V FITC Apoptosis detection Kit (eBioscience) following the manufacturer's protocol. In brief, cells were detached from the plate using TrypLETM Express and washed once in PBS and once in 1x binding buffer. Thereafter the cells were resuspended in 1x binding buffer (1-5 x 10^6 cells/ml) and 5 μl of FITC-Annexin V were added to 100 μl of this cell suspension. After an incubation for 10-15 min at room temperature the cells were washed once again with 1x binding buffer and subsequently resuspended in 200 μl 1x binding buffer. After the addition of 5 μl of propidium iodide staining solution the cells were analyzed by flow cytometry within 4 h.

Colony formation assays

5 x 10^5 cells were seeded on a 10 cm plate, followed by a treatment with CPT as specified in the figure legend. Afterwards the medium was removed, cells were washed with PBS and cells were grown in complete DMEM medium for further 2 days. Then the cells were washed with PBS, fixed with ice-cold methanol for 10 min and stained with 0.5% (w/v) crystal violet

(in 25% ethanol) for 10 min. The excess dye was removed by rinsing the cells twice with distilled water and the plates were photographed.

Monoclonal anti-HIPK2 and anti-HIPK3 antibodies

The development of HIPK2 monoclonal antibodies was done as described (de la Vega *et al.*, 2013) and one of the clones recognizing HIPK2 with a high affinity (C-5C6, rat IgG2a) was used in this study. To develop monoclonal antibodies recognizing HIPK3, the region encompassing sequences between amino acids 881-1050 of human HIPK3 was expressed as a His-tagged protein in *E.coli*. The HIPK3 fragment was purified under denaturing conditions and dialyzed against PBS. 50 µg of the purified protein was injected intraperitoneally (i.p.) and subcutaneously (s.c.) into LOU/C rats using incomplete Freund's adjuvant supplemented with 5 nmol CpG 2006 (TIB MOLBIOL, Berlin, Germany). After a six weeks interval a final boost with 50 µg HIPK3 protein was given i.p. and s.c. three days before fusion. Fusions of the myeloma cell line P3X63-Ag8.653 with the rat immune spleen cells were performed according to standard procedures. Hybridoma supernatants were tested in a solid-phase immunoassay with HIPK3 coated to ELISA plates. Antibodies from tissue culture supernatant bound to HIPK3 were detected with HRP conjugated mAbs against the rat IgG isotypes (TIB173 IgG2a, TIB174 IgG2b, TIB170 IgG1 all from ATCC, R-2c IgG2c homemade), thus avoiding mAbs of IgM class. HRP was visualized with ready to use TMB (1-StepTM Ultra TMB-ELISA, Thermo Fisher). MAbs that reacted specifically with HIPK3 were further analyzed in Western blotting. The clones 5C1 (R-G1) and 19A8 (R-G1) were selected and subsequently used for Western blotting.

Acknowledgements

We are grateful to Dr. Elisa Izaurralde (Tübingen) for helpful discussions, the plasmids for tethering assays and antibodies recognizing CNOT1. We thank all colleagues who have generously provided plasmids, especially Dres. O.S. Gabrielsen (Oslo), J.J. Palvimo (Helsinki), M. Timmers (Utrecht), S. Winkler (Nottingham), F. Zhang (Boston), R. Singh (Ames) and S. Hoshino (Nagoya). We are also indebted to Dr. Issay Kitabayashi (Tokyo) for sharing HIPK2-deficient MEFs. This work was supported by grants from the Deutsche Forschungsgemeinschaft (SCHM 1417/8-3, SCHM 1417/9-1), Deutsche Krebshilfe (111447), FB/TRR81, SFB1021 and the Excellence Cluster Cardio-Pulmonary System (ECCPS).

References

Aulas, A., Caron, G., Gkogkas, C.G., Mohamed, N.V., Destroismaisons, L., Sonenberg, N., Leclerc, N., Parker, J.A., and Vande Velde, C. (2015). G3BP1 promotes stress-induced RNA granule interactions to preserve polyadenylated mRNA. The Journal of cell biology *209*, 73-84.

Babbarwal, V., Fu, J., and Reese, J.C. (2014). The Rpb4/7 module of RNA polymerase II is required for carbon catabolite repressor protein 4-negative on TATA (Ccr4-not) complex to promote elongation. The Journal of biological chemistry *289*, 33125-33130.

Bartlam, M., and Yamamoto, T. (2010). The structural basis for deadenylation by the CCR4-NOT complex. Protein Cell *1*, 443-452.

Boland, A., Chen, Y., Raisch, T., Jonas, S., Kuzuoglu-Ozturk, D., Wohlbold, L., Weichenrieder, O., and Izaurralde, E. (2013). Structure and assembly of the NOT module of the human CCR4-NOT complex. Nature structural & molecular biology *20*, 1289-1297.

Buchan, J.R., and Parker, R. (2009). Eukaryotic stress granules: the ins and outs of translation. Molecular cell *36*, 932-941.

Collart, M.A., and Panasenko, O.O. (2012). The Ccr4--not complex. Gene *492*, 42-53.

Cooke, A., Prigge, A., and Wickens, M. (2010). Translational repression by deadenylases. The Journal of biological chemistry *285*, 28506-28513.

Cox, J., and Mann, M. (2008). MaxQuant enables high peptide identification rates, individualized p.p.b.-range mass accuracies and proteome-wide protein quantification. Nature biotechnology *26*, 1367-1372.
D'Orazi, G., Cecchinelli, B., Bruno, T., Manni, I., Higashimoto, Y., Saito, S., Gostissa, M., Coen, S., Marchetti, A., Del Sal, G., Piaggio, G., Fanciulli, M., Appella, E., and Soddu, S. (2002). Homeodomain-interacting protein kinase-2 phosphorylates p53 at Ser 46 and mediates apoptosis. Nat Cell Biol *4*, 11-19.
D'Orazi, G., Rinaldo, C., and Soddu, S. (2012). Updates on HIPK2: a resourceful oncosuppressor for clearing cancer. J Exp Clin Cancer Res *31*, 63.
de la Vega, L., Frobius, K., Moreno, R., Calzado, M.A., Geng, H., and Schmitz, M.L. (2011). Control of nuclear HIPK2 localization and function by a SUMO interaction motif. Biochimica et biophysica acta *1813*, 283-297.
de la Vega, L., Grishina, I., Moreno, R., Kruger, M., Braun, T., and Schmitz, M.L. (2012). A redox-regulated SUMO/acetylation switch of HIPK2 controls the survival threshold to oxidative stress. Molecular cell *46*, 472-483.
de la Vega, L., Hornung, J., Kremmer, E., Milanovic, M., and Schmitz, M.L. (2013). Homeodomain-interacting protein kinase 2-dependent repression of myogenic differentiation is relieved by its caspase-mediated cleavage. Nucleic Acids Res *41*, 5731-5745.
Dumont, A., Hehner, S.P., Hofmann, T.G., Ueffing, M., Droge, W., and Schmitz, M.L. (1999). Hydrogen peroxide-induced apoptosis is CD95-independent, requires the release of mitochondria-derived reactive oxygen species and the activation of NF-kappaB. Oncogene *18*, 747-757.
Dutta, A., Babbarwal, V., Fu, J., Brunke-Reese, D., Libert, D.M., Willis, J., and Reese, J.C. (2015). Ccr4-Not and TFIIS Function Cooperatively To Rescue Arrested RNA Polymerase II. Molecular and cellular biology *35*, 1915-1925.
Gehring, N.H., Hentze, M.W., and Kulozik, A.E. (2008). Tethering assays to investigate nonsense-mediated mRNA decay activating proteins. Methods Enzymol *448*, 467-482.
Hofmann, T.G., Glas, C., and Bitomsky, N. (2013). HIPK2: A tumour suppressor that controls DNA damage-induced cell fate and cytokinesis. BioEssays : news and reviews in molecular, cellular and developmental biology *35*, 55-64.
Hofmann, T.G., Moller, A., Sirma, H., Zentgraf, H., Taya, Y., Droge, W., Will, H., and Schmitz, M.L. (2002). Regulation of p53 activity by its interaction with homeodomain-interacting protein kinase-2. Nat Cell Biol *4*, 1-10.
Hölper, S., Nolte, H., Bober, E., Braun, T., and Kruger, M. (2015). Dissection of metabolic pathways in the Db/Db mouse model by integrative proteome and acetylome analysis. Molecular bioSystems *11*, 908-922.
Houghton, P.J., Cheshire, P.J., Hallman, J.D., 2nd, Lutz, L., Friedman, H.S., Danks, M.K., and Houghton, J.A. (1995). Efficacy of topoisomerase I inhibitors, topotecan and irinotecan, administered at low dose levels in protracted schedules to mice bearing xenografts of human tumors. Cancer chemotherapy and pharmacology *36*, 393-403.
Houseley, J., and Tollervey, D. (2009). The many pathways of RNA degradation. Cell *136*, 763-776.
Isono, K., Nemoto, K., Li, Y., Takada, Y., Suzuki, R., Katsuki, M., Nakagawara, A., and Koseki, H. (2006). Overlapping roles for homeodomain-interacting protein kinases hipk1 and hipk2 in the mediation of cell growth in response to morphogenetic and genotoxic signals. Mol Cell Biol *26*, 2758-2771.
Ito, K., Inoue, T., Yokoyama, K., Morita, M., Suzuki, T., and Yamamoto, T. (2011). CNOT2 depletion disrupts and inhibits the CCR4-NOT deadenylase complex and induces apoptotic cell death. Genes Cells *16*, 368-379.

Jeck, W.R., Sorrentino, J.A., Wang, K., Slevin, M.K., Burd, C.E., Liu, J., Marzluff, W.F., and Sharpless, N.E. (2013). Circular RNAs are abundant, conserved, and associated with ALU repeats. RNA *19*, 141-157.
Kerr, S.C., Azzouz, N., Fuchs, S.M., Collart, M.A., Strahl, B.D., Corbett, A.H., and Laribee, R.N. (2011). The Ccr4-Not complex interacts with the mRNA export machinery. PloS one *6*, e18302.
Kim, Y.H., Choi, C.Y., Lee, S.J., Conti, M.A., and Kim, Y. (1998). Homeodomain-interacting protein kinases, a novel family of co-repressors for homeodomain transcription factors. J Biol Chem *273*, 25875-25879.
Laribee, R.N., Shibata, Y., Mersman, D.P., Collins, S.R., Kemmeren, P., Roguev, A., Weissman, J.S., Briggs, S.D., Krogan, N.J., and Strahl, B.D. (2007). CCR4/NOT complex associates with the proteasome and regulates histone methylation. Proceedings of the National Academy of Sciences of the United States of America *104*, 5836-5841.
Lassus, P., Ferlin, M., Piette, J., and Hibner, U. (1996). Anti-apoptotic activity of low levels of wild-type p53. The EMBO journal *15*, 4566-4573.
Lau, N.C., Kolkman, A., van Schaik, F.M., Mulder, K.W., Pijnappel, W.W., Heck, A.J., and Timmers, H.T. (2009). Human Ccr4-Not complexes contain variable deadenylase subunits. The Biochemical journal *422*, 443-453.
Lau, N.C., Mulder, K.W., Brenkman, A.B., Mohammed, S., van den Broek, N.J., Heck, A.J., and Timmers, H.T. (2010). Phosphorylation of Not4p functions parallel to BUR2 to regulate resistance to cellular stresses in Saccharomyces cerevisiae. PloS one *5*, e9864.
Lazzari, C., Prodosmo, A., Siepi, F., Rinaldo, C., Galli, F., Gentileschi, M., Bartolazzi, A., Costanzo, A., Sacchi, A., Guerrini, L., and Soddu, S. (2011). HIPK2 phosphorylates DeltaNp63alpha and promotes its degradation in response to DNA damage. Oncogene *30*, 4802-4813.
Lemaire, M., and Collart, M.A. (2000). The TATA-binding protein-associated factor yTafII19p functionally interacts with components of the global transcriptional regulator Ccr4-Not complex and physically interacts with the Not5 subunit. The Journal of biological chemistry *275*, 26925-26934.
Li, X., Luo, Y., Yu, L., Lin, Y., Luo, D., Zhang, H., He, Y., Kim, Y.O., Kim, Y., Tang, S., and Min, W. (2008). SENP1 mediates TNF-induced desumoylation and cytoplasmic translocation of HIPK1 to enhance ASK1-dependent apoptosis. Cell Death Differ *15*, 739-750.
Lin, J., Zhang, Q., Lu, Y., Xue, W., Xu, Y., Zhu, Y., and Hu, X. (2014). Downregulation of HIPK2 increases resistance of bladder cancer cell to cisplatin by regulating Wip1. PloS one *9*, e98418.
Maryati, M., Airhihen, B., and Winkler, G.S. (2015). The enzyme activities of Caf1 and Ccr4 are both required for deadenylation by the human Ccr4-Not nuclease module. The Biochemical journal.
Milanovic, M., Kracht, M., and Schmitz, M.L. (2014). The cytokine-induced conformational switch of nuclear factor kappaB p65 is mediated by p65 phosphorylation. The Biochemical journal *457*, 401-413.
Miller, J.E., and Reese, J.C. (2012). Ccr4-Not complex: the control freak of eukaryotic cells. Critical reviews in biochemistry and molecular biology *47*, 315-333.
Moriya, H., Shimizu-Yoshida, Y., Omori, A., Iwashita, S., Katoh, M., and Sakai, A. (2001). Yak1p, a DYRK family kinase, translocates to the nucleus and phosphorylates yeast Pop2p in response to a glucose signal. Genes Dev *15*, 1217-1228.
Norbeck, J. (2008). Carbon source dependent dynamics of the Ccr4-Not complex in Saccharomyces cerevisiae. Journal of microbiology *46*, 692-696.
Ohnheiser, J., Ferlemann, E., Haas, A., Muller, J.P., Werwein, E., Fehler, O., Biyanee, A., and Klempnauer, K.H. (2015). Programmed cell death 4 protein (Pdcd4) and homeodomain-

interacting protein kinase 2 (Hipk2) antagonistically control translation of Hipk2 mRNA. Biochimica et biophysica acta *1853*, 1564-1573.
Panasenko, O.O., and Collart, M.A. (2011). Not4 E3 ligase contributes to proteasome assembly and functional integrity in part through Ecm29. Molecular and cellular biology *31*, 1610-1623.
Preissler, S., Reuther, J., Koch, M., Scior, A., Bruderek, M., Frickey, T., and Deuerling, E. (2015). Not4-dependent translational repression is important for cellular protein homeostasis in yeast. The EMBO journal *34*, 1905-1924.
Radhakrishnan, S.K., and Kamalakaran, S. (2006). Pro-apoptotic role of NF-kappaB: implications for cancer therapy. Biochimica et biophysica acta *1766*, 53-62.
Renner, F., Saul, V.V., Pagenstecher, A., Wittwer, T., and Schmitz, M.L. (2011). Inducible SUMO modification of TANK alleviates its repression of TLR7 signalling. EMBO reports *12*, 129-135.
Reuven, N., Adler, J., Porat, Z., Polonio-Vallon, T., Hofmann, T.G., and Shaul, Y. (2015). The Tyrosine Kinase c-Abl Promotes Homeodomain-interacting Protein Kinase 2 (HIPK2) Accumulation and Activation in Response to DNA Damage. The Journal of biological chemistry *290*, 16478-16488.
Russell, P., Benson, J.D., and Denis, C.L. (2002). Characterization of mutations in NOT2 indicates that it plays an important role in maintaining the integrity of the CCR4-NOT complex. J Mol Biol *322*, 27-39.
Sakamoto, K., Huang, B.W., Iwasaki, K., Hailemariam, K., Ninomiya-Tsuji, J., and Tsuji, Y. (2010). Regulation of genotoxic stress response by homeodomain-interacting protein kinase 2 through phosphorylation of cyclic AMP response element-binding protein at serine 271. Mol Biol Cell *21*, 2966-2974.
Saul, V.V., de la Vega, L., Milanovic, M., Krüger, M., Braun, T., Fritz-Wolf, K., Becker, K., and Schmitz, M.L. (2013). HIPK2 kinase activity depends on cis-autophosphorylation of its activation loop. J Mol Cell Biol *5*, 27-38.
Saul, V.V., and Schmitz, M.L. (2013). Posttranslational modifications regulate HIPK2, a driver of proliferative diseases. J Mol Med (Berl) *91*, 1051-1058.
Schmitz, M.L., Rodriguez-Gil, A., and Hornung, J. (2014). Integration of stress signals by homeodomain interacting protein kinases. Biol Chem *395*, 375-386.
Shang, Y., Doan, C.N., Arnold, T.D., Lee, S., Tang, A.A., Reichardt, L.F., and Huang, E.J. (2013). Transcriptional corepressors HIPK1 and HIPK2 control angiogenesis via TGF-beta-TAK1-dependent mechanism. PLoS Biol *11*, e1001527.
Shi, J., and Nelson, M.A. (2005). The cyclin-dependent kinase 11 interacts with NOT2. Biochemical and biophysical research communications *334*, 1310-1316.
Siepi, F., Gatti, V., Camerini, S., Crescenzi, M., and Soddu, S. (2013). Homeodomain-interacting protein kinase 2 (HIPK2) catalytic activity and specificity are regulated by activation-loop Y354 autophosphorylation. Biochim Biophys Acta *1833*, 1443-1453.
Smeenk, L., van Heeringen, S.J., Koeppel, M., Gilbert, B., Janssen-Megens, E., Stunnenberg, H.G., and Lohrum, M. (2011). Role of p53 serine 46 in p53 target gene regulation. PLoS One *6*, e17574.
Tucker, M., Valencia-Sanchez, M.A., Staples, R.R., Chen, J., Denis, C.L., and Parker, R. (2001). The transcription factor associated Ccr4 and Caf1 proteins are components of the major cytoplasmic mRNA deadenylase in Saccharomyces cerevisiae. Cell *104*, 377-386.
van der Laden, J., Soppa, U., and Becker, W. (2015). Effect of tyrosine autophosphorylation on catalytic activity and subcellular localisation of homeodomain-interacting protein kinases (HIPK). Cell communication and signaling : CCS *13*, 3.
Vousden, K.H. (2006). Outcomes of p53 activation--spoilt for choice. Journal of cell science *119*, 5015-5020.

Zekri, L., Kuzuoglu-Ozturk, D., and Izaurralde, E. (2013). GW182 proteins cause PABP dissociation from silenced miRNA targets in the absence of deadenylation. The EMBO journal *32*, 1052-1065.
Zhang, Q., Nottke, A., and Goodman, R.H. (2005). Homeodomain-interacting protein kinase-2 mediates CtBP phosphorylation and degradation in UV-triggered apoptosis. Proceedings of the National Academy of Sciences of the United States of America *102*, 2802-2807.

Figure legends

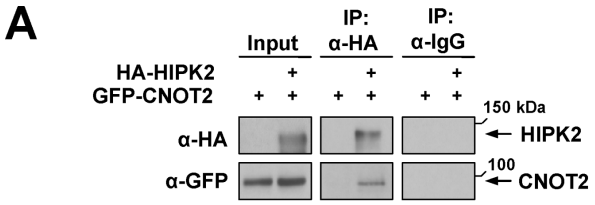
A
Input
IP: α-HA
IP: α-IgG
HA-HIPK2
GFP-CNOT2
150 kDa
α-HA
HIPK2
α-GFP
100
CNOT2

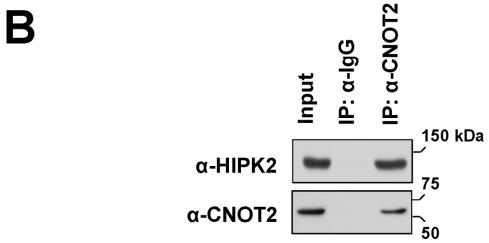
B
Input
IP: α-IgG
IP: α-CNOT2
150 kDa
α-HIPK2
75
α-CNOT2
50

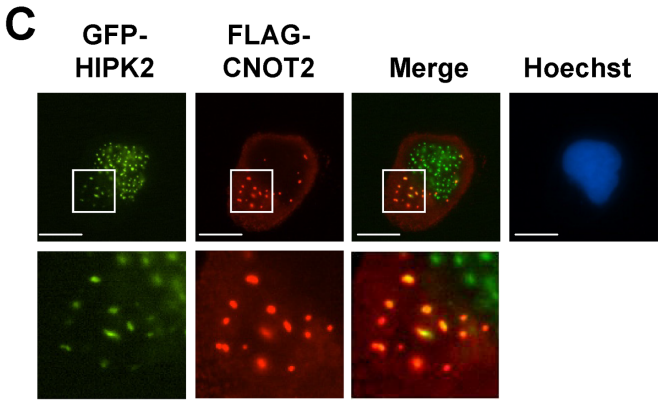
C
GFP-HIPK2
FLAG-CNOT2
Merge
Hoechst

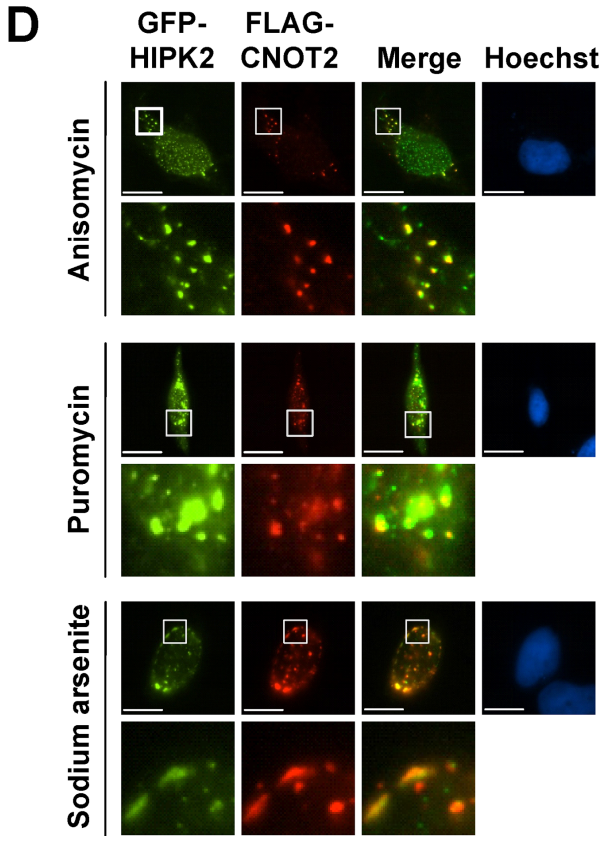
D
GFP-HIPK2
FLAG-CNOT2
Merge
Hoechst
Anisomycin
Puromycin
Sodium arsenite

Figure 1. HIPK2 and CNOT2 interact and co-localize in cytosolic speckles. (**A**) 293T cells were transfected with GFP-CNOT2 either alone or in combination with HA-HIPK2. 24 h post transfection cells were lysed and proteins were immunoprecipitated (IP) using an anti-HA antibody or a control rat IgG antibody. Precipitated samples were analyzed by Western blotting using appropriate antibodies, input samples of the cell lysates were analyzed for correct protein expression. The positions of molecular weight markers are indicated. (**B**) Cells were treated for 30 min with a cell permeable crosslinker to preserve protein/protein interactions occurring in intact cells. After removal of the crosslinker and quenching, cells were lysed and subjected to immunoprecipitation using control or anti-CNOT2 antibodies. The precipitates and input controls were analyzed by immunoblotting. (**C**) U2OS cells co-expressing GFP-HIPK2 and FLAG-CNOT2 were stained and analyzed by indirect immunofluorescence to reveal the localization of HIPK2 and CNOT2, nuclear DNA was stained by Hoechst. The scale bar is 10 μM, the area indicated by white boxes is displayed in the lower panel in 5x magnification. The merge shows areas of co-localization in yellow. (**D**) HeLa cells expressing GFP-HIPK2 and FLAG-CNOT2 were treated with anisomycin (10 μg/ml for 30 min), puromycin (100 μg/ml for 60 min) or sodium arsenite (0.5 mM for 60 min). The cells were fixed and analyzed by immunofluorescence as shown, yellow color in the merged images indicates co-localization of the two proteins. The scale bar is 10 μM, the boxed area is displayed in the lower panel in 5x magnification.

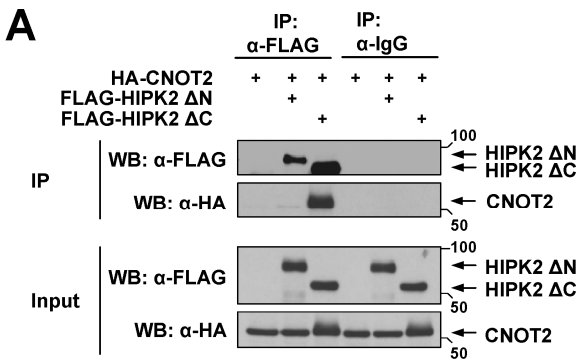
A
IP: α-FLAG
IP: α-IgG
HA-CNOT2
FLAG-HIPK2 ΔN
FLAG-HIPK2 ΔC
IP
WB: α-FLAG
WB: α-HA
Input
WB: α-FLAG
WB: α-HA
100
50
HIPK2 ΔN
HIPK2 ΔC
CNOT2

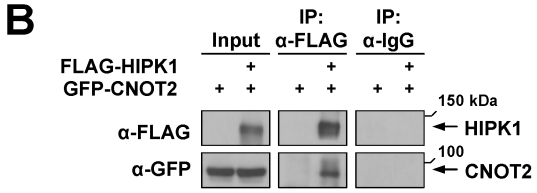
B
Input
IP: α-FLAG
IP: α-IgG
FLAG-HIPK1
GFP-CNOT2
α-FLAG
α-GFP
150 kDa
HIPK1
100
CNOT2

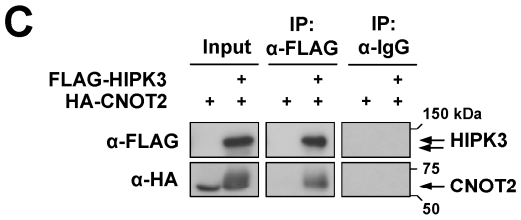
C
Input
IP: α-FLAG
IP: α-IgG
FLAG-HIPK3
HA-CNOT2
α-FLAG
α-HA
150 kDa
HIPK3
75
CNOT2
50

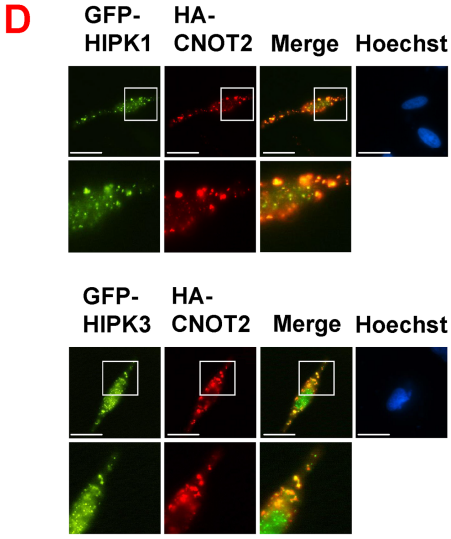
D
GFP-HIPK1
HA-CNOT2
Merge
Hoechst
GFP-HIPK3
HA-CNOT2
Merge
Hoechst

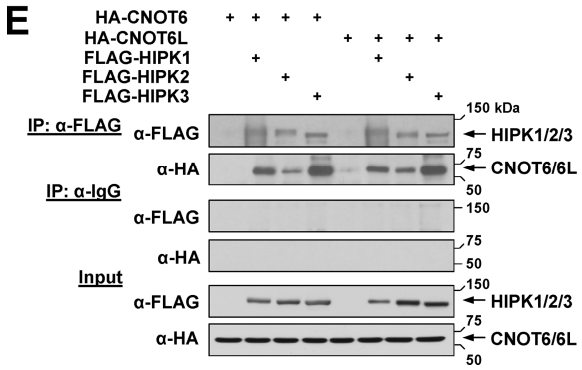
E
HA-CNOT6
HA-CNOT6L
FLAG-HIPK1
FLAG-HIPK2
FLAG-HIPK3
IP: α-FLAG
α-FLAG
α-HA
IP: α-IgG
α-FLAG
α-HA
Input
α-FLAG
α-HA
150 kDa
HIPK1/2/3
75
CNOT6/6L
50
150
75
50
150
HIPK1/2/3
75
CNOT6/6L
50

Figure 2. CNOT2 binds to HIPKs. (**A**) 293T cells were transfected to express HA-CNOT2 alone or in combination with either FLAG-HIPK2 ΔN or FLAG-HIPK2 ΔC. An aliquot of the lysates was analyzed for correct protein expression (Input), another aliquot was used for co-immunoprecipitation using anti-FLAG antibody or an isotype-matched control mouse IgG antibody. Samples were analyzed by Western blotting as shown. (**B**) The indicated plasmids encoding FLAG-HIPK1 or GFP-CNOT2 were transfected into 239T cells and lysates were used either for input controls or co-immunoprecipitation with the indicated antibodies as displayed. (**C**) The experiment was done as in (B) with the difference that HA-CNOT2 and FLAG-HIPK3 were co-expressed. (**D**) HeLa cells co-expressing HA-CNOT2 and GFP-tagged HIPKs were stained and analyzed by indirect immunofluorescence to reveal the localization of HIPK1/3 and CNOT2, nuclear DNA was stained by Hoechst. The scale bar is 10 μM, the area indicated by white boxes is displayed in the lower panel in 5x magnification. The merge shows areas of co-localization in yellow. (**E**) 293T cells were transfected with the indicated plasmids coding for epitope-tagged CNOT6/6L, HIPK1, HIPK2 and HIPK3. Cells were lysed and lysates were analyzed for correct protein expression (Input). Immunoprecipitation was performed using anti-FLAG antibody or a control mouse IgG antibody. Precipitated proteins and input samples were separated by SDS-PAGE and analyzed by Western blotting using appropriate antibodies.

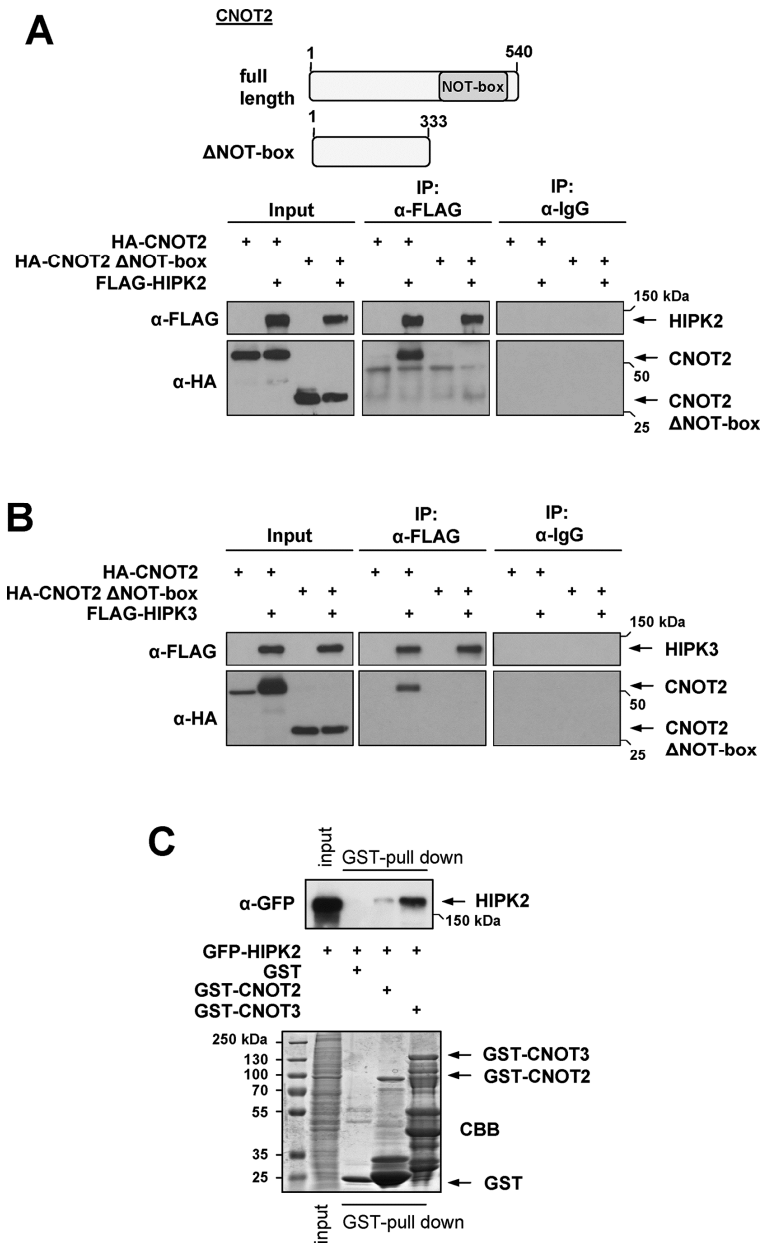

Figure 3. The NOT-box in CNOT2 is important for HIPK binding. (**A**) Upper: Schematic representation of CNOT2 and the CNOT2 deletion mutant ΔNOT-box. Lower: The HA-tagged CNOT2 and CNOT2 ΔNOT-box proteins were co-expressed with FLAG-HIPK2 as shown, followed by cell extraction and analysis of proteins for expression (input) and mutual binding by co-immunoprecipitation as shown. (**B**) The experiment was done as in (A) with the exception that binding to HIPK3 was measured. (**C**) Cells transfected to express GFP-HIPK2 were lysed and extracts were tested for interaction with bacterially produced GST, GST-CNOT2 and GST-CNOT3 proteins by pull-down experiments as shown. The upper part shows a Western blot displaying the input material and the eluates. The lower part shows the CBB-stained input material and GST fusion proteins used for this experiment.

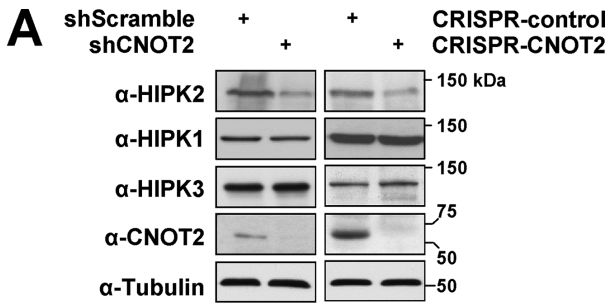
A
shScramble + +
shCNOT2 + +
CRISPR-control
CRISPR-CNOT2
α-HIPK2
α-HIPK1
α-HIPK3
α-CNOT2
α-Tubulin
150 kDa
150
150
75
50
50

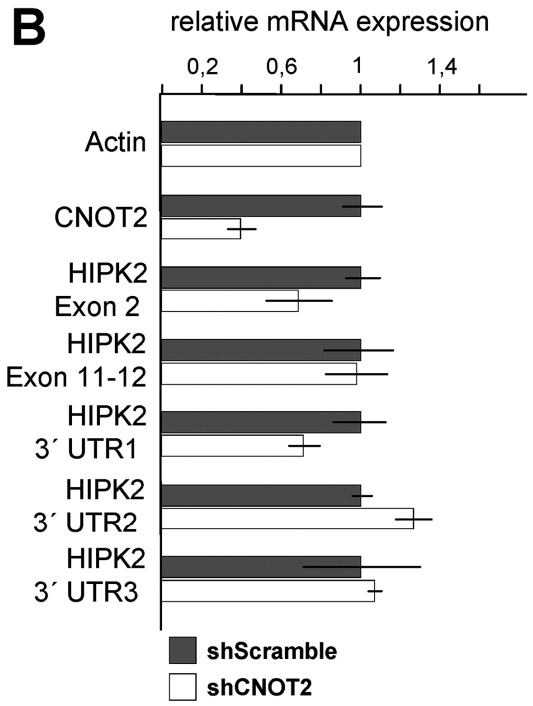
B
relative mRNA expression
0,2
0,6
1
1,4
Actin
CNOT2
HIPK2 Exon 2
HIPK2 Exon 11-12
HIPK2 3´ UTR1
HIPK2 3´ UTR2
HIPK2 3´ UTR3
shScramble
shCNOT2

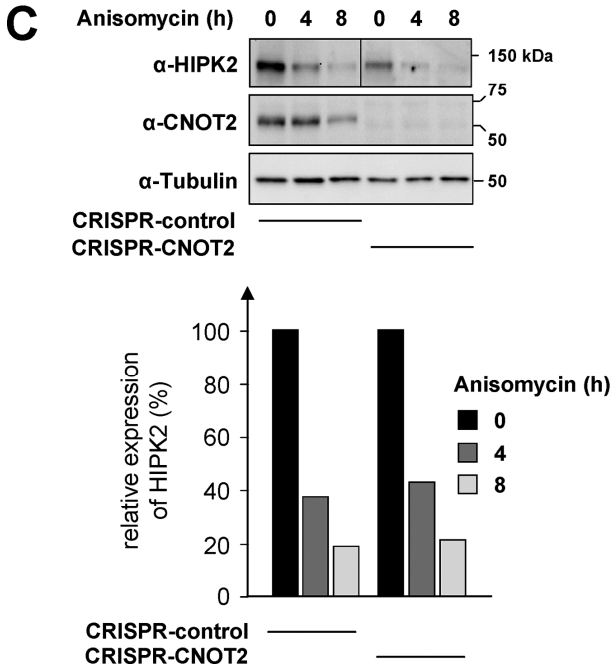
C
Anisomycin (h) 0 4 8 0 4 8
α-HIPK2
α-CNOT2
α-Tubulin
150 kDa
75
50
50
CRISPR-control
CRISPR-CNOT2
relative expression of HIPK2 (%)
100
80
60
40
20
0
Anisomycin (h)
0
4
8
CRISPR-control
CRISPR-CNOT2

Figure 4. Regulation of HIPK2 protein amounts by CNOT2. (**A**) Expression of the CNOT2 protein was either partially reduced by the expression of a specific shRNA or completely prohibited by CRISPR-Cas9-mediated genome engineering. Cell extracts were prepared and equal amounts of proteins analyzed for the expression of all HIPKs and the indicated controls as shown. (**B**) 293T cells transfected to express a CNOT2 specific shRNA or a scrambled control were analyzed for HIPK2 mRNA levels by qPCR. Five different primer pairs were used to quantify HIPK2 mRNA at different exons and the 3´ untranslated region (3´ UTR) as shown. Values were normalized to the housekeeping gene β-actin and relative expression levels were determined using the ΔΔCt method. Error bars show standard deviations from two independent experiments performed in triplicates. (**C**) Upper: The protein stability of HIPK2 was compared between control 293T cells and a cell line where CNOT2 expression was eliminated by CRISPR-Cas9-mediated gene editing. The cells were treated with anisomycin or vehicle for the indicated periods as shown. Equal numbers of cells were lysed and lysates were analyzed for protein expression by immunoblotting. Lower: The HIPK2 protein expression levels were quantified using the Chemidoc touch imaging system (Biorad). To facilitate comparison, the protein levels in the respective vehicle controls were arbitrarily set as 100%.

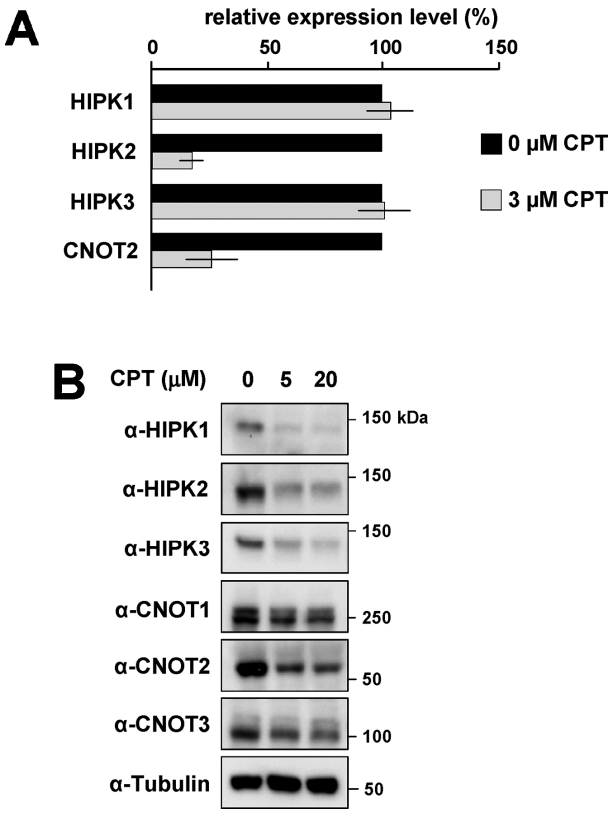

Figure 5. CPT-mediated downregulation of CNOT2 and HIPK2. (**A**) 293T cells were treated with indicated concentrations of CPT for 16 h. Total RNA was isolated and mRNA levels of the indicated genes were analyzed with real-time qPCR using gene specific primers. Error bars display the standard deviations from two independent experiments. (**B**) Cells were treated for 24 h with different concentrations of CPT and the levels of the indicated proteins were detected by Western blot analysis using specific antibodies.

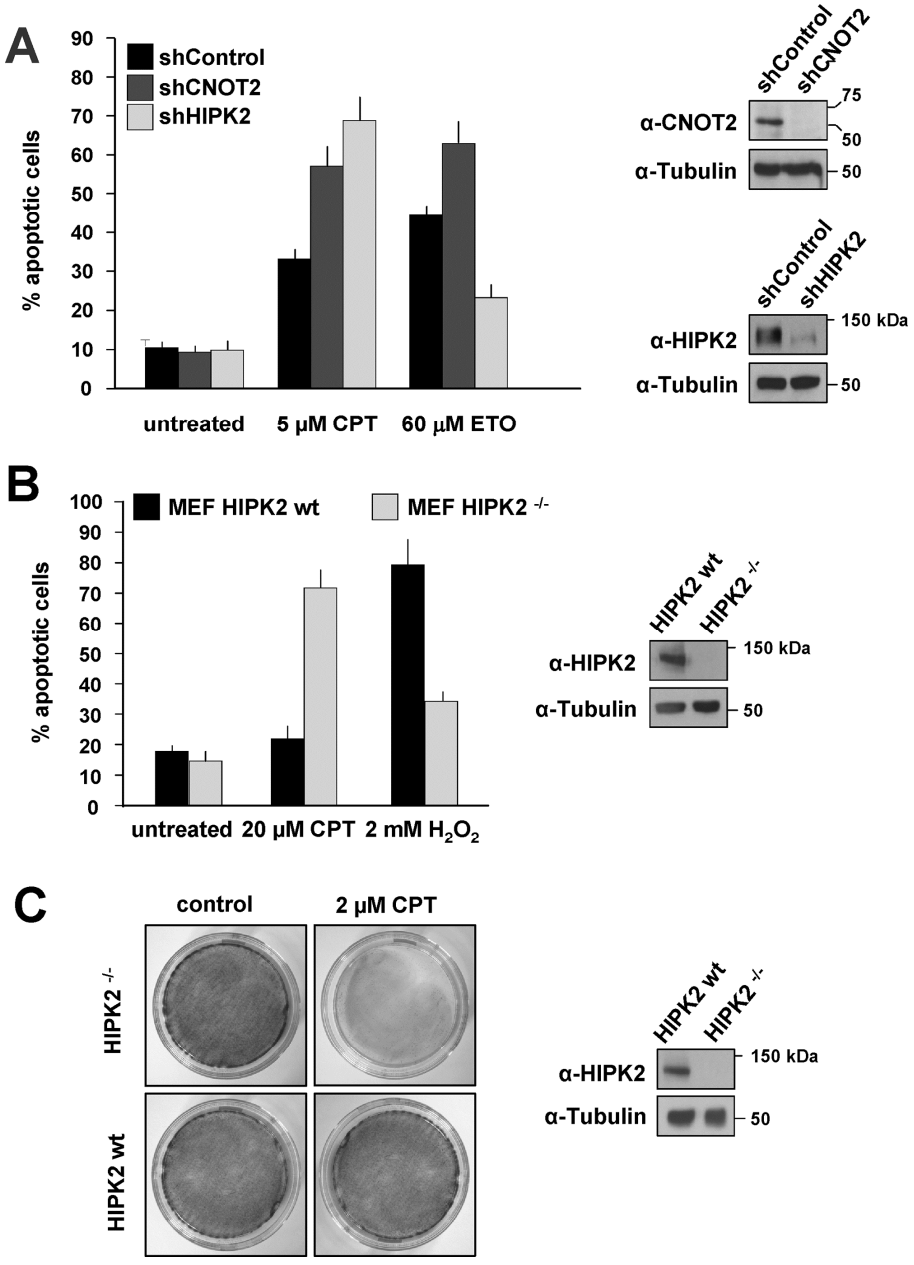

Figure 6. HIPK2 depletion sensitizes cells towards CPT-induced apoptosis. (**A**) 293T cells were transfected with vectors directing the expression of HIPK2- or CNOT2-specific shRNAs or an unspecific control shRNA. Transfected cells were selected for two days in puromycin to eliminate untransfected cells. Subsequently 5 µM CPT or 60 µM etoposide were added for 24 h. Most of the cells were used to measure apoptosis in the flow cytometer using the Annexin V Apoptosis detection Kit FITC, error bars show standard deviations from two independent experiments performed in triplicates. An aliquot of the cells was used to control the knockdown efficiencies by Western blotting. (**B**) HIPK2 knockout MEFs reconstituted either with an empty vector ($HIPK2^{-/-}$) or with HIPK2 wildtype (HIPK2 wt) were treated with 20 µM CPT or 2 mM hydrogen peroxide for 24 h. Apoptosis was measured in the flow cytometer, results show a quantification of cell death, error bars indicate standard deviations from two independent experiments performed in triplicates. An aliquot of cells was used as a control to ensure HIPK2 expression (right). (**C**) Equal numbers of the HIPK2 knockout and

reconstituted MEFs used in (B) were seeded in 10 cm dishes. After addition of 2 µM CPT for 24 h, cells were washed twice and complete DMEM was added for 2 days. Cells were fixed and subsequently stained with crystal violet, a representative experiment is shown. The right part displays a control Western blot ensuring correct HIPK2 expression.

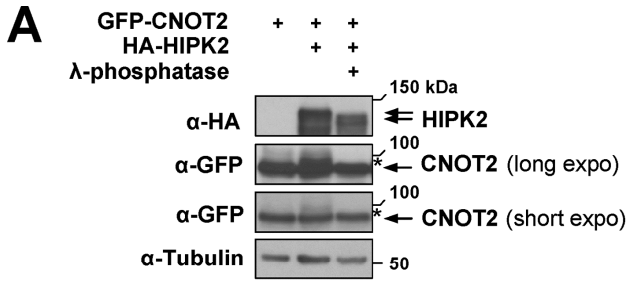
A
GFP-CNOT2 + + +
HA-HIPK2 + +
λ-phosphatase +
150 kDa
α-HA
HIPK2
100
α-GFP
CNOT2 (long expo)
100
α-GFP
CNOT2 (short expo)
α-Tubulin
50

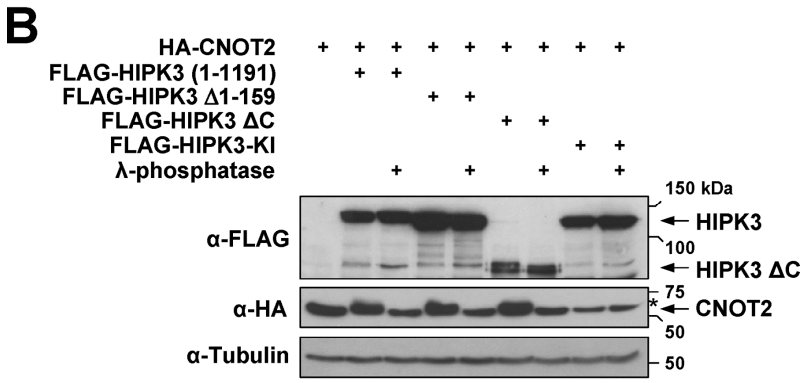
B
HA-CNOT2 + + + + + + + + +
FLAG-HIPK3 (1-1191) + +
FLAG-HIPK3 Δ1-159 + +
FLAG-HIPK3 ΔC + +
FLAG-HIPK3-KI + +
λ-phosphatase + + + +
150 kDa
α-FLAG
HIPK3
100
HIPK3 ΔC
75
α-HA
CNOT2
50
α-Tubulin
50

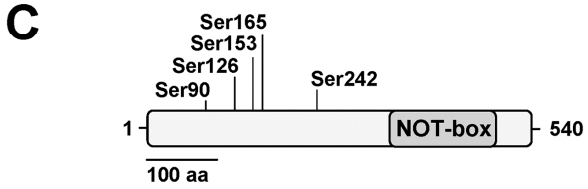
C
Ser165
Ser153
Ser126
Ser90
Ser242
1
NOT-box
540
100 aa

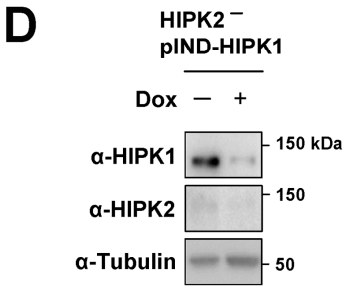
D
HIPK2 −
pIND-HIPK1
Dox − +
α-HIPK1
150 kDa
α-HIPK2
150
α-Tubulin
50

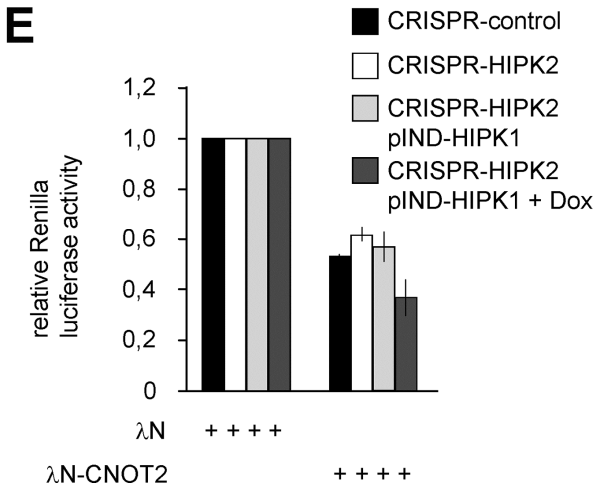
E
CRISPR-control
CRISPR-HIPK2
CRISPR-HIPK2
pIND-HIPK1
CRISPR-HIPK2
pIND-HIPK1 + Dox
relative Renilla
luciferase activity
1,2
1,0
0,8
0,6
0,4
0,2
0
λN + + + +
λN-CNOT2 + + + +

Figure 7. Phosphorylation and regulation of CNOT2. (**A**) 293T cells were transfected to express epitope-tagged CNOT2 together with full length HIPK2. Cell lysates were treated with λ-phosphatase for 30 min as indicated and analyzed by Western blotting using appropriate antibodies. Two different exposure times for the detection of CNOT2 are shown, the phosphorylated form is marked by a star. (**B**) HA-CNOT2 was co-expressed along with HIPK3 or the indicated variants thereof including a kinase inactive point mutant (FLAG-HIPK3 KI). Cell lysates were treated with λ-phosphatase as indicated and proteins were analyzed by Western blot with appropriate antibodies. The phosphorylated forms are marked by a star. (**C**) Schematic representation of CNOT2 indicating the positions of the identified HIPK phosphorylation sites. (**D**) HIPK2 CRISPR-Cas9 knockout cells characterized in supplementary Fig. 7A were stably transfected with pIND-HIPK1 and cells were treated for 3 days with doxycycline (1 μg/ml) to allow downregulation of HIPK1. Cells were characterized by Western blotting as shown. (**E**) The indicated cells were left untreated or treated with doxycycline (1 μg/ml) for 2 days. Cells were then transfected with the Renilla luciferase reporter plasmid containing 5 B-boxes in its 3´ UTR along with the λN expression vectors (50 ng) and the Firefly luciferase used for normalization. Cells were grown for further 24 h in the absence or presence of doxycycline and luciferase activities were determined. To facilitate comparison the luciferase activity in the presence λN was set as 1, error bars indicate standard deviations obtained from two independent experiments performed in triplicates.

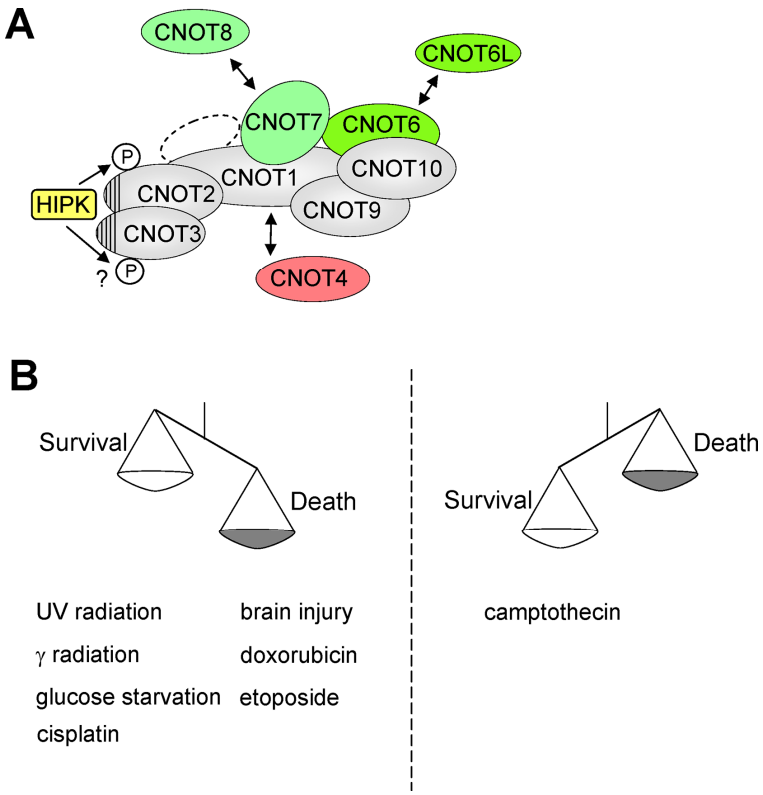

Figure 8. Schematic models summarizing the results. (**A**) Association with and phosphorylation by the HIPKs is shown schematically. The NOT-boxes contained in CNOT2 and CNOT3 are indicated by striated areas. The subunits with deadenylation activity are shown in green, the loosely associated subunit with ubiquitin E3 ligase activity is shown in red. (**B**) Schematic model showing the pro- and anti-apoptotic functions of HIPK2.

Supplemental Materials

Molecular Biology of the Cell

Rodriguez-Gil et al.

Supplementary Information

Supplementary Table 3

Antibodies

Primary antibody (clone)	Species	Supplier
anti-Flag (M2)	mouse mAb	Sigma
anti-GFP (7.1 and 13.1)	mouse mAbs	Roche
anti-HA (3F10)	rat mAb	Roche
anti-HIPK1 (ab90103)	Rabbit pAb	Abcam
anti-HIPK2	rat 5C6 mAb	self-made
anti-HIPK3	rat 5C1 mAb	self-made
anti-HIPK3	rat 19A8 mAb	self-made
anti- CNOT2 (2191C2a)	mouse mAbs	Santa Cruz
anti-AKT (#9272)	rabbit pAb	Cell Signaling
anti-Tubulin (Tub2.1)	mouse mAb	Sigma
anti-PARP (C-2-10)	mouse mAb	Sigma

Plasmids

Plasmid	Origin	Reference
HA-HIPK2	Schmitz lab	EMBO J. 2010 Nov 17;29(22):3750-61.
GFP-HIPK2	Schmitz lab	EMBO J. 2010 Nov 17;29(22):3750-61.
Flag-HIPK2 ΔN	Schmitz lab	Nat Cell Biol. 2002 Jan;4(1):1-10.
Flag-HIPK2 ΔC	Schmitz lab	Nat Cell Biol. 2002 Jan;4(1):1-10.
Flag-HIPK1 (1-1191)	O.S. Gabrielsen (Oslo)	Biochem Biophys Res Commun. 2009 Oct 9;388(1):150-4.
Flag-HIPK3 ΔC	J.J. Palvimo (Helsinki)	Mol Biol Cell. 1998 Sep;9(9):2527-43.
Flag-HIPK3 Δ1-159	this study	
Flag-HIPK3-KI	J.J. Palvimo (Helsinki)	Mol Biol Cell. 1998 Sep;9(9):2527-43.
GFP-CNOT2	M. Timmers (Utrecht)	Nucleic Acids Res. 2000 Feb 1;28(3):809-17.
Flag-CNOT2	this study	
HA-CNOT2	this study	
HA-CNOT2 ΔNOT-box	this study	
HA-CNOT6	S. Winkler (Nottingham)	Mol Biol Cell. 2011 Mar 15;22(6):748-58.

HA-CNOT6L	S. Winkler (Nottingham)	Mol Biol Cell. 2011 Mar 15;22(6):748-58.
GST-CNOT2	this study	
GST-CNOT3	this study	
pSUPER-shCNOT2	this study	
pSUPER-shScramble	Schmitz lab	EMBO J. 2010 Nov 17;29(22):3750-61.
pX459	F. Zhang (Boston)	Nat Protoc. 2013 Nov;8(11):2281-308
pX459-CNOT2	this study	
pX459-HIPK2	this study	
Gal4-HIPK2	Schmitz lab	EMBO J. 2010 Nov 17;29(22):3750-61.
AD-CNOT2	this study	
Flag-TIA1	R. Singh (Ames)	Mol Cell Biol. 2011 Mar;31(5):935-54.
Flag-Pan3	S. Hoshino (Nagoya)	Genes Dev. 2007 Dec 1;21(23):3135-48.
pINDUCER-CNOT1	this study	
pINDUCER-CNOT2	this study	
pINDUCER-Luci	this study	
pINDUCER-HIPK1	this study	
pQE-Tri His-Strep1-HIPK3 (881-1050)	this study	
pClneo-RLuc-5BoxB	E.Izaurralde	Genes Dev. 2006 Jul 15;20(14):1885-98.
pClneo-N3FLuc	E.Izaurralde	Genes Dev. 2006 Jul 15;20(14):1885-98.
pClneo-LambdaN-HA	E.Izaurralde	Genes Dev. 2006 Jul 15;20(14):1885-98.
pClneo-LambdaN-HA-CNOT2 + point mutants	this study	

DNA Oligonucleotides

Oligo name	Sequence (5´ to 3´)
huActin-qPCR-f	TCCCTGGAGAAGAGCTACGA
huActin-qPCR-r	AGGAAGGAAGGCTGGAAGAG
HIPK1 -f	AGCTGCTCAGCCACTACAGA
HIPK1 -r	GGTGTGATGGTGGCTACTTG
HIPK2 E2-f	CCTACCTTACGAGCAGACCAT
HIPK2 E2-r	CTTGCCCGGTGACAGAAGT
HIPK2 E11-12-f	AGGAAGAGTAAGCAGCACCAG
HIPK2	TGCTGATGGTGATGACACTGA

E11-12-r	
HIPK2 3´UTR1-f	GTCGGGACACCAGTGAAACT
HIPK2 3´UTR1-r	GGCGTAGAATGGGTTCTTGA
HIPK2 3´UTR2-f	AAATGGCTCGGTGCTCTCAA
HIPK2 3´UTR2-r	AGACAGGGAATGAAGCCTGC
HIPK2 3´UTR3-f	TTGTCATCCACCTCACCACG
HIPK2 3´UTR3-r	ACGTGGTCAAAGCAAAACGG
qHIPK3 -f	GAATGCTTTCAGCACCGTAA
qHIPK3 -r	ATGGGCCGAATCACTTTTAG
qCNOT2 _F	TTGGAATGATTGGCCTGTTA
qCNOT2 _R	CGCAAATTTGGGGTAGAGAT
miRE-Xho-fw	TGAACTCGAGAAGGTATATTGCTGTTGACAGTGAGCG
miRE-Eco-rev	TCTCGAATTCTAGCCCCTTGAAGTCCGAGGCAGTAGGC
miR-Luci	TGCTGTTGACAGTGAGCGcccgcctgaagtctctgattaaTAGTGAAGCCACAGATGT AttaatcagagacttcaggcggtTGCCTACTGCCTCGGA
miR-CNOT1	TGCTGTTGACAGTGAGCGcggcttccaagatatagcaataTAGTGAAGCCACAGATGT AtattgctatatcttggaagccaTGCCTACTGCCTCGGA
miR-CNOT2	TGCTGTTGACAGTGAGCGacatctggaatatgacaaattaTAGTGAAGCCACAGATGT AtaatttgtcatattccagatggTGCCTACTGCCTCGGA
miR-HIPK1	TGCTGTTGACAGTGAGCGcacaccctcaagtagccaccataTAGTGAAGCCACAGAT GTAtatggtggctacttgagggtggTGCCTACTGCCTCGGA

Reagents

Reagent	Supplier
Anisomycin	Sigma-Aldrich
Puromycin	Invitrogen
Sodium Arsenite	Sigma-Aldrich
dimethyl-3-3'-dithiobispropionimidate 2-HCl	Pierce
GSH Sepharose	GE Healthcare Life sciences
λ phosphatase	New England Biolabs
Camptothecin	Sigma-Aldrich
Hydrogen peroxide	Sigma-Aldrich
Hoechst 33342	Invitrogen

Supplementary Figures

Supplementary Figure 1

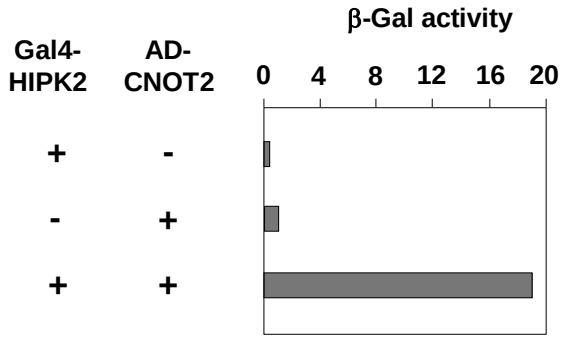

Supplementary Fig. 1. The yeast strain AH109 was transformed either with the bait vector alone (pGBKT7 where the DNA-binding domain of Gal4 was fused to kinase inactive HIPK2), the prey vector (pACT2 where CNOT2 was fused to the acidic transactivation domain of Gal4) or both plasmids together. The expression of β-galactosidase (given in Miller units) was measured according to the manual provided by the manufacturer (Clontech).

Supplementary Figure 2

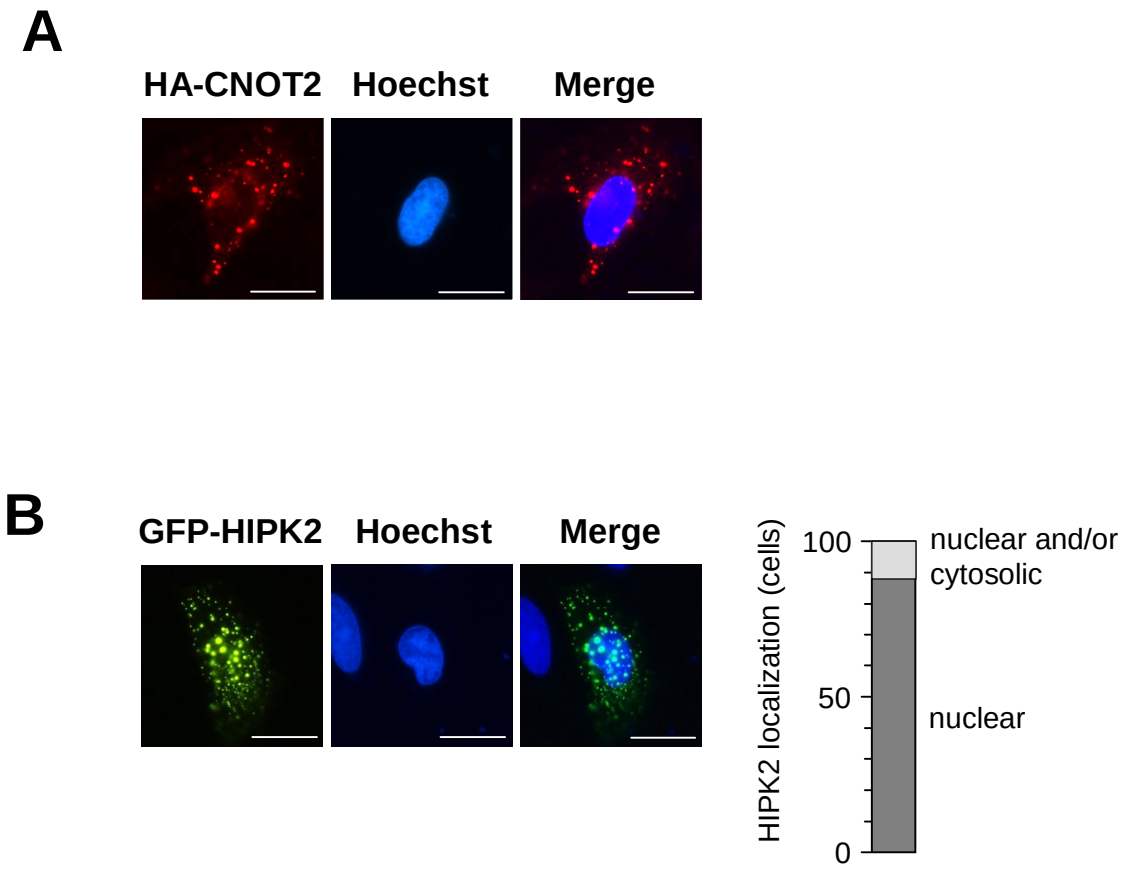

Supplementary Fig. 2. HeLa cells were transfected to express HA-CNOT2 (A) or GFP-HIPK2 (B). After 1 day the intracellular localization of CNOT2 was determined by indirect immunofluorescence and GFP-HIPK2 was detected by the intrinsic fluorescence of GFP. Nuclear DNA was stained by Hoechst, the scale bar is 10 μM. The right part shows a quantitative analysis of HIPK2 localization in 100 healthy interphase cells.

Supplementary Figure 3

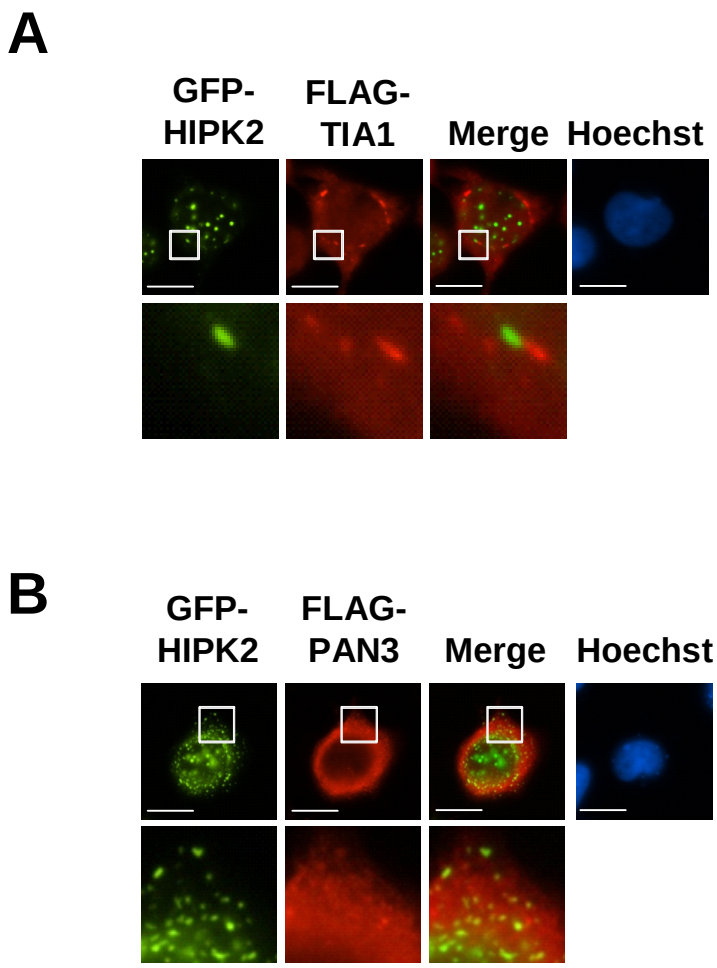

Supplementary Fig. 3. Cytosolic HIPK2 foci do not co-localize with the stress granule marker TIA1 or the P-body marker PAN3. (A) GFP-HIPK2 and either FLAG-TIA1 or (B) FLAG-PAN3 were co-expressed in HeLa cells and stained with an anti-FLAG antibody and a Cy3-coupled secondary antibody. Nuclear DNA was stained with Hoechst 33324. Scale bar is 10 μM, the area indicated by white boxes is displayed in the lower panel in five-fold magnification.

Supplementary Figure 4

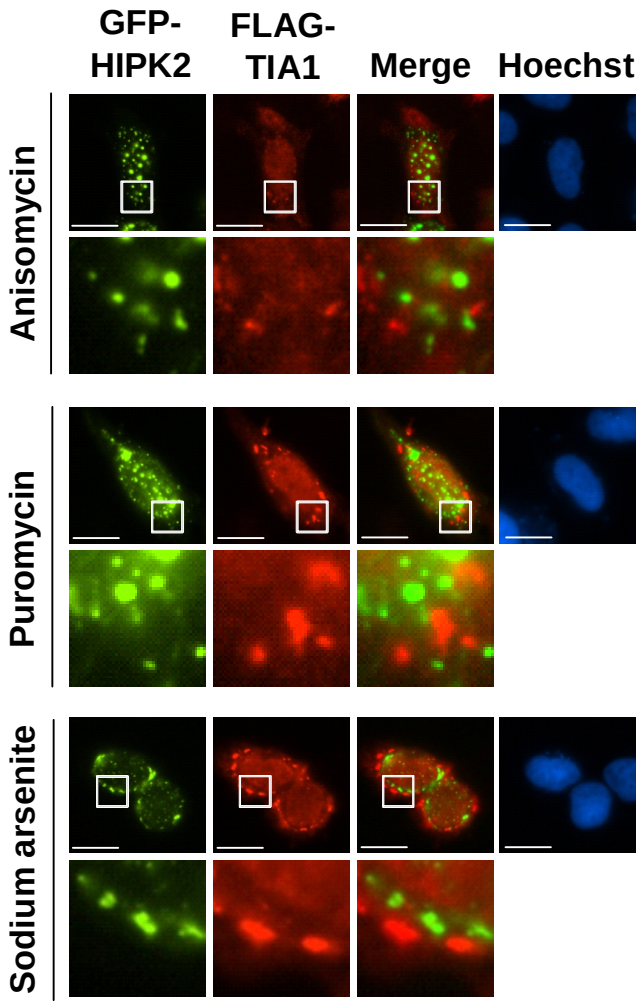

Supplementary Fig. 4. HeLa cells expressing GFP-HIPK2 and FLAG-TIA1 were treated with Anisomycin (10 µg/ml for 30 min), Puromycin (100 µg/ml for 60 min) or sodium arsenite (0.5 mM for 60 min). The cells were fixed and analyzed by immunofluorescence as shown. The boxed area is displayed in the lower panel in five-fold magnification, the scale bar is 10 µM.

Supplementary Figure 5

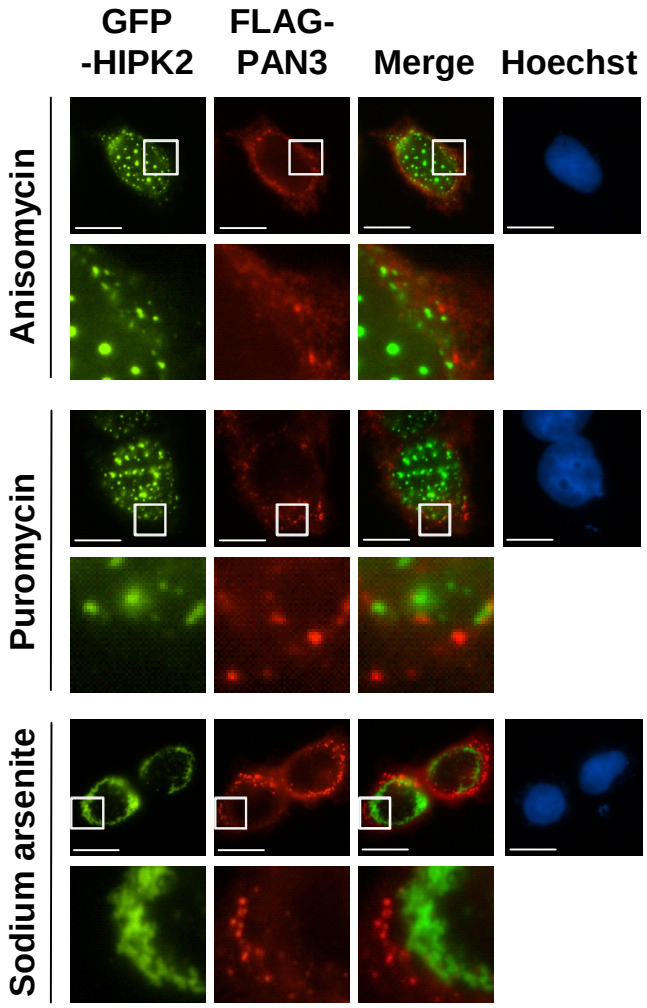

Supplementary Fig. 5. GFP-HIPK2 and FLAG-PAN3 were co-expressed in HeLa cells. 24 h later the cells were treated with Anisomycin, Puromycin or sodium arsenite as described in supplementary Fig. 3. Thereafter cells were fixed and stained with an anti-FLAG and a Cy3-coupled secondary antibody; nuclear DNA was stained with Hoechst 33324. The boxed area is displayed in the lower panel in five-fold magnification, the scale bar is 10 μM.

Supplementary Figure 6

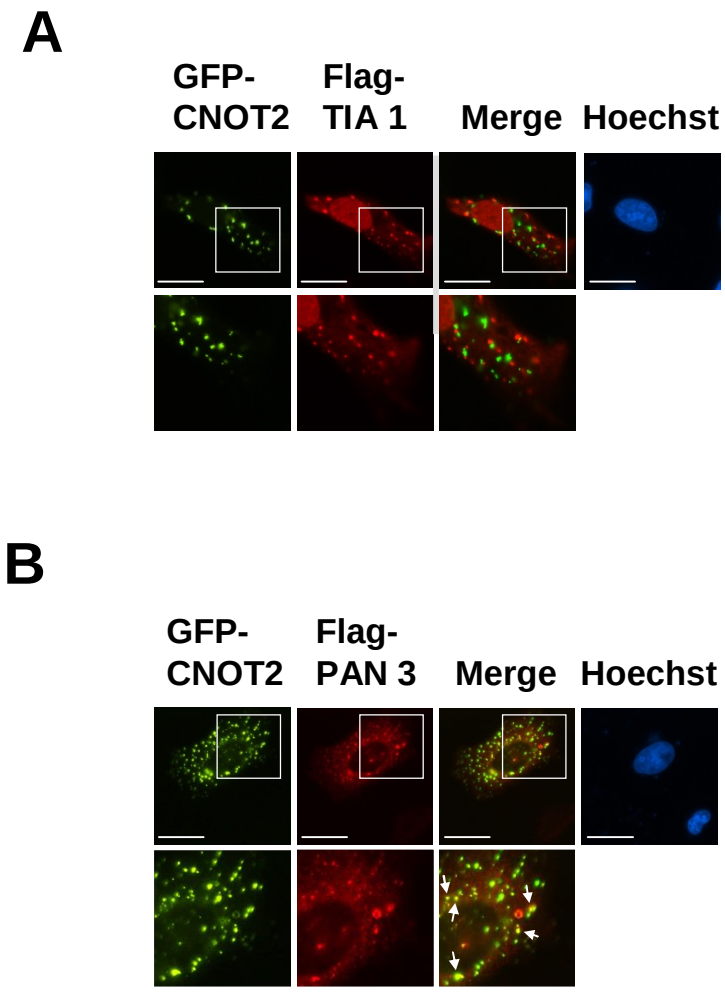

Supplementary Fig. 6. HeLa cells were transfected to express GFP-CNOT2 together with Flag-TIA1 (A) or Flag-Pan3 (B). The intracellular localization of the proteins is shown, the nuclear DNA was stained with Hoechst. The scale bar is 10 μM, the area indicated by white boxes is displayed in the lower panel in 5x magnification. Areas of co-localization in the merge appear in yellow and are indicated by arrows.

Supplementary Figure 7

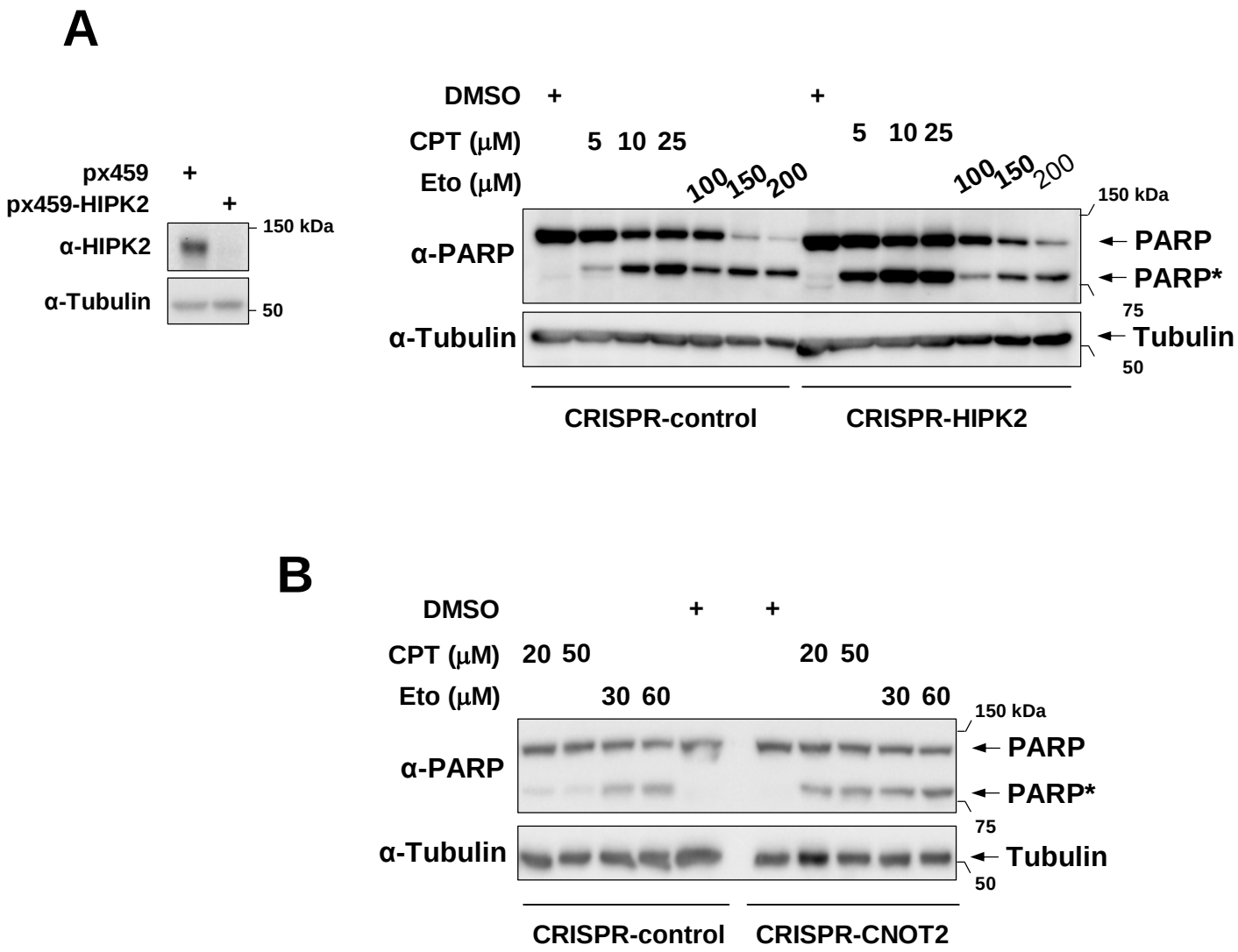

Supplementary Fig. 7. (**A**) HeLa cells were transfected with the vectors px459 or px459-HIPK2. Transfected cells were selected by puromycin treatment and surviving clones were grown to colonies. A fraction of the cells was lysed and equal amounts of protein were tested by immunoblotting for expression levels of HIPK2 and Tubulin with specific antibodies. A cell clone with a deletion of HIPK2 is displayed in the left. The control cell clone and the HIPK2-deficient cell clone were treated for 24 h (CPT) or 48 h (Eto) with the indicated concentrations of the DNA damaging agents. Cell lysates were analyzed for the caspase-mediated cleavage of poly ADP-ribose polymerase (PARP) to the 85 kDa cleavage product (indicated as PARP*). (B) The experiment was done as in (A) with the difference that control 293T cells and CNOT2 knockout cells were compared for CPT- or Eto-induced PARP cleavage.

Supplementary Figure 8

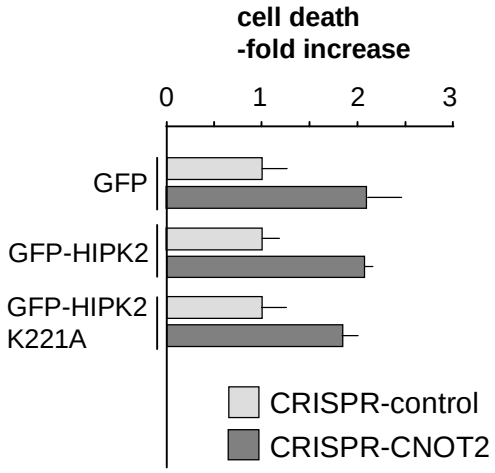

Supplementary Fig. 8. Control 293T cells and CNOT2 knockout 293T cells were transfected to express GFP, GFP-HIPK2 or kinase inactive GFP-HIPK2 K221A. After 36 h the cells were treated for 24 h with CPT (20 μM) and cell death was determined by FACS by gating for GFP-positive and PI-positive cells. Error bars show standard deviations from an experiment performed in triplicates.

Supplementary Figure 9

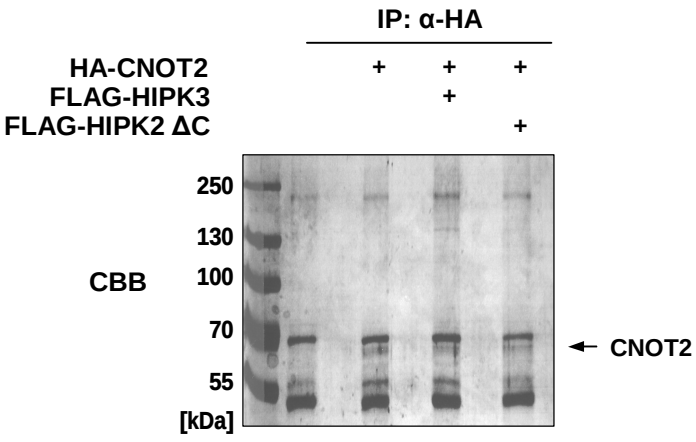

Supplementary Fig. 9. Purification of phosphorylated CNOT2 protein. HA-CNOT2 was co-expressed with FLAG-HIPK2 ΔC or FLAG-HIPK3 in 293T cells and purified by immunoprecipitation using anti-HA antibodies. Eluted proteins were separated by SDS-PAGE and analyzed by CBB staining to confirm successful purification of CNOT2 which is indicated by an arrow. The positions of molecular weight marker proteins are displayed.

Supplementary Figure 10

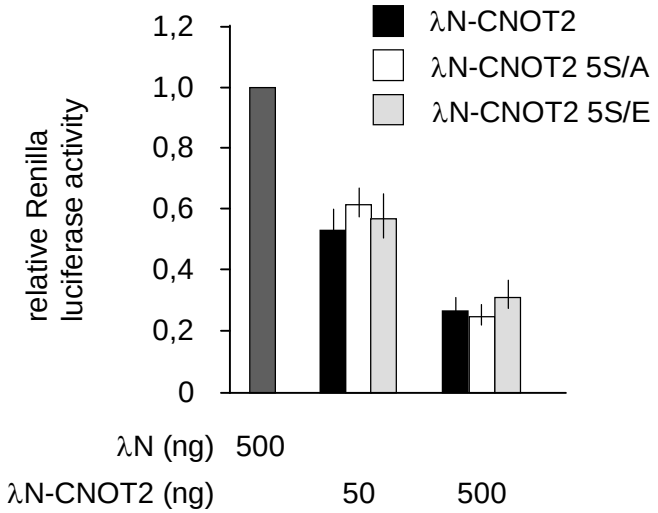

Supplementary Fig. 10. CNOT2-deficient 293T cells were transfected with the Renilla luciferase reporter plasmid containing 5 B-boxes in its 3´ UTR along with the indicated amounts of λN and λN-CNOT2 expression vectors encoding wildtype CNOT2 or mutants where all 5 phosphorylation sites were changed to alanine (5S/A) or to glutamic acid (5S/E) together with a plasmid encoding the Firefly luciferase used for normalization. Cells were grown for further 24 h and luciferase activities were determined. To facilitate comparison, the luciferase activity in the presence λN was set as 1, error bars indicate standard deviations obtained from an experiment performed in triplicates.

Supplementary Figure 11

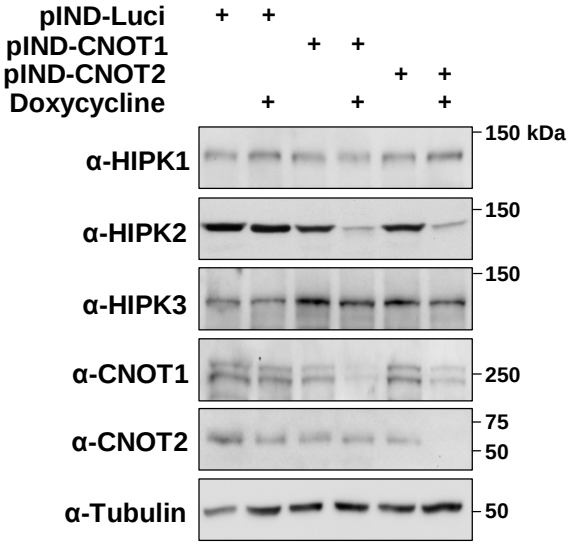

Supplementary Fig. 11. Stable 293T cell lines allowing the doxycycline-inducible expression of shRNAs for luciferase (control), CNOT1 or CNOT2 were treated for 2 days with doxycycline. Cell extracts were prepared and equal amounts of proteins were analyzed by immunoblotting for the indicated proteins as shown. Molecular weight markers are indicated.

Supplementary Table 1.

HIPK2-mediated phosphorylation of CNOT2				
Position	**Modified Sequence**	**Score Diff**	**Localization Probability**	**PEP**
Ser90	_GM(ox)**S(ph)**NNTPQINR_	47,8173	0,999983	0,0004074
Ser126	_SIS(ph)QGTQIPSHVTPTTGVPTM(ox)SIHTPP**S(ph)**PSR_	14,1075	0,939693	6,33E-24
Ser153	_NM(ox)M(ox)NHSQVGQGIGIP**S(ph)**R_	56,2139	0,999998	3,95E-11
Ser165	_TNSMSSSGIG**S(ph)**PNR_	12,6904	0,947285	2,33E-10
Ser242	_REG**S(ph)**GNPTPIINPIAGR_	12,9586	0,951838	2,20E-33
HIPK3-mediated phosphorylation of CNOT2				
Position	**Modified Sequence**	**Score Diff**	**Localization Probability**	**PEP**
Ser90	_GM(ox)**S(ph)**NNTPQINR_	75,2688	1	7,39E-18
Ser126	_SIS(ph)QGTQIPSHVTPTTGVPTM(ox)SIHTPP**S(ph)**PSR_	6,04833	0,8083	7,67E-24
Ser153	_NM(ox)M(ox)NHSQVGQGIGIP**S(ph)**R_	147,102	1	1,66E-06
Ser165	_TNSMSSSGIG**S(ph)**PNR_	18,6162	0,986305	1,23E-09
Ser242	_REG**S(ph)**GNPTPIINPIAGR_	51,4743	0,999993	2,80E-16

Supplementary Table 1. List of HIPK2 and HIPK3-dependent CNOT2 phosphorylation sites. 239T cells were transfected to express HA-tagged CNOT2 alone or CNOT2 together with either HIPK2 or HIPK3. After cell lysis and immunoprecipitation of HA-tagged CNOT2 the proteins were separated by one-dimensional SDS-PAGE (4-12% Novex-gels, Invitrogen) and stained with colloidal Coomassie. HA-CNOT2 gel bands were excised and subjected to in gel-digest with trypsin. The resulting tryptic peptides were extracted with acetonitrile, desalted and analyzed by mass spectrometry using a nano-flow HPLC system (Proxeon) connected to a LTQ-Orbitrap-XL and LTQ-orbitrap Velos instrument (Thermo Fisher Scientific) equipped with a nanoelectrospray source (Proxeon). The HIPK-dependent phosphorylation sites in CNOT2 are displayed.